Biogeosciences Discuss., 12, 12543–12610, 2015
www.biogeosciences-discuss.net/12/12543/2015/
doi:10.5194/bgd-12-12543-2015

Biogeosciences Discussions
Open Access

Looking beyond stratification: a model-based analysis of the biological drivers of oxygen depletion in the North Sea

F. Große[1], N. Greenwood[2,3], M. Kreus[4], H. J. Lenhart[1], D. Machoczek[5], J. Pätsch[6], L. A. Salt[7], and H. Thomas[8]

[1]University of Hamburg, Department of Informatics, Scientific Computing, Bundesstraße 45a, 20146 Hamburg, Germany
[2]Centre for Environment, Fisheries and Aquaculture Science (Cefas), Lowestoft, Suffolk, NR33 0HT, UK
[3]University of East Anglia, School of Environmental Sciences, Norwich, NR4 7TJ, UK
[4]University of Hamburg, Institute for Hydrobiology and Fisheries Science, Olbersweg 24, 22767 Hamburg, Germany
[5]Federal Maritime and Hydrographic Agency, Bernhard-Nocht-Straße 78, 20359 Hamburg, Germany
[6]University of Hamburg, CEN, Institute of Oceanography, Bundesstraße 53, 20146 Hamburg, Germany

[7]CNRS, UMR 7144, Equipe Chimie Marine, Station Biologique de Roscoff, Place Georges Teissier, 29680, Roscoff, France
[8]Dalhousie University, Department of Oceanography, 1355 Oxford Street, Halifax, Canada

Received: 30 June 2015 – Accepted: 12 July 2015 – Published: 10 August 2015

Correspondence to: F. Große (fabian.grosse@uni-hamburg.de)

Published by Copernicus Publications on behalf of the European Geosciences Union.

BGD
12, 12543–12610, 2015

Abstract

The problem of low oxygen conditions, often referred to as hypoxia, occurs regularly in the North Sea, a temperate European shelf sea. Stratification represents a major process regulating the seasonal dynamics of bottom oxygen. However, lowest oxygen conditions in the North Sea do not occur in the regions of strongest stratification. This suggests that stratification is an important prerequisite for hypoxia, but that the complex interaction between hydrodynamics and the biological processes drives its development.

In this study we use the ecosystem model HAMSOM-ECOHAM5 to provide a general characteristic of the different North Sea oxygen regimes, and to quantify the impact of the different physical and biological factors driving the oxygen dynamics below the thermocline and in the bottom layer.

We show that the North Sea can be subdivided into three different regimes in terms of oxygen dynamics: (1) a highly productive, non-stratified coastal regime, (2) a productive, seasonally stratified regime with a small sub-thermocline volume, and (3) a productive, seasonally stratified regime with a large sub-thermocline volume, with regime 2 being highly susceptible to hypoxic conditions.

Our analysis of the different processes driving the oxygen development reveals that inter-annual variations in the oxygen conditions are caused by variations in primary production, while spatial differences can be attributed to differences in stratification and water depth. In addition, we show that benthic bacteria represent the main oxygen consumers in the bottom layer, consistently accounting for more than 50 % of the overall consumption.

By providing these valuable insights, we show that ecosystem models can be a useful tool for the interpretation of observations and the estimation of the impact of anthropogenic drivers on the North Sea oxygen conditions.

BGD
12, 12543–12610, 2015

1 Introduction

The problem of low oxygen (O_2) conditions, often referred to as hypoxia, occurs regularly in the North Sea. A major process regulating the seasonal dynamics of bottom O_2 is the occurrence and duration of thermal stratification (e.g. Greenwood et al., 2010; O'Boyle and Nolan, 2010), which limits the vertical exchange of O_2 between the oxygenated surface layer and the deeper layers, and separates the productive and respiratory regimes of the water column (surface and subsurface). Both effects favour in synergy the occurrence of O_2 depletion events (e.g. Diaz and Rosenberg, 2008). However, even though the northern North Sea reveals strongest stratification, lowest O_2 concentrations occur in the central North Sea, where the duration of stratification is shorter and shows highest inter-annual variability. Thus, one can argue that stratification is an important prerequisite for hypoxia, but the severity and duration of low O_2 conditions is controlled by the complex interaction between the hydrodynamical condition and the biogeochemical processes involved.

The North Sea is a temperate, semi-enclosed shelf sea adjacent to the northeastern Atlantic ocean. It has an average depth of about 90 m (Ducrotoy et al., 2000) with northward increasing bottom depth. The North Sea circulation is characterised by a cyclonic pattern mainly driven by the southward Atlantic inflow across the shelf edge defining its northern boundary. Lenhart and Pohlmann (1997) showed that about 85 % of the incoming Atlantic water is recirculated north of the Dogger Bank, a shallow area with water depth less than 40 m and 300 km of zonal extent at about 55° N, 2° E (Kröncke and Knust, 1995). The circulation south of the Dogger Bank is governed by the inflow through the English Channel and follows the continental coast. Northwest of Denmark it joins the Norwegian coastal current leaving the North Sea at its northern boundary.

Stratification in the North Sea reveals some significant regional differences. While the shallower southern parts are permanently well-mixed due to the strong influence of the M_2 tidal component (Otto et al., 1990), the deeper parts north of 54° N reveal seasonal, mostly thermal stratification (e.g. Burt et al., 2014; Pingree et al., 1978; van

BGD
12, 12543–12610, 2015

Leeuwen et al., 2015). Seasonal haline stratification occurs to a lesser extent along the Norwegian coast. The transition between these permanently mixed and seasonally stratified regions occurs gradually (Pingree et al., 1978). In consequence, even areas relatively near to the coast, which are affected by high riverine nutrient run-off, often reveal stratified conditions at sub-seasonal timescales (e.g. Burt et al., 2014).

The events of O_2 depletion, occurring regularly in the southeastern and southern central North Sea under stratified conditions (Brockmann and Eberlein, 1986; Brockmann et al., 1990; Queste et al., 2013; Rachor and Albrecht, 1983), can be classified as "persistent seasonal" according to Kemp et al. (2009). The problem of low O_2 conditions in the North Sea reached public awareness in relation to the eutrophication problem during the 1980s, when demersal animals died across a large area due to low O_2 concentrations (v. Westernhagen et al., 1986). Eutrophication, or in other words, high anthropogenic nutrient loads mainly supplied by rivers (Brockmann et al., 1988; Jickells, 1998; Rabalais et al., 2010), may raise the ambient nutrient concentrations followed by an increase in biomass production. Under given physical conditions, eutrophication thus causes an enhanced supply of organic matter sinking into the subsurface layer and thus reinforces O_2 consumption near the sea floor due to bacterial remineralisation.

Even though the second International Conference on the Protection of the North Sea (INSC-2) prescribed a 50 %-reduction of river nutrient loads in order to mitigate the effects of eutrophication (de Jong, 2006), low bottom O_2 concentrations remain a persistent problem in the North Sea up to the present day as shown in Fig. 1. The ecological disturbance of different levels of low O_2 concentration is summarized and described in detail, for instance, by Friedrich et al. (2014) and Topcu et al. (2009). Low bottom O_2 concentrations may lead to the death of benthic organisms or fish eggs as well as avoidance of the affected areas by benthic species. Therefore, low O_2 concentration constitutes a major indicator of eutrophication (category 3 indicator, i.e. "evidence of undesirable disturbance"; OSPAR-Commission, 2003) and O_2 concentrations

BGD
12, 12543–12610, 2015

lower than 6 mg L^{-1} result in the classification as so-called "problem area" in terms of eutrophication within the OSPAR assessment (Claussen et al., 2009).

Despite the relevance of the bottom O_2 concentration for the assessment of the ecological status of an ecosystem, O_2 measurements are sparse and either temporally or spatially limited. In addition, it is difficult to place the measurement at the right time and location to obtain a comprehensive picture of the duration and spatial extent of O_2 depletion events (Friedrich et al., 2014). One way to address this problem is to analyse the available data towards their confidence level with respect to eutrophication assessment (Brockmann and Topcu, 2014).

Only in recent years continuous measurements for the North Sea became available by, for instance, the SmartBuoy programme of Cefas (Centre for Environment, Fisheries and Aquaculture Science, UK; Greenwood et al., 2010) or the MARNET programme (MARine Monitoring NETwork in the North Sea and Baltic Sea) of the BSH (Federal Maritime and Hydrographic Agency, Germany). These monitoring programmes provide daily time series of O_2 and related parameters (e.g. temperature, salinity, chlorophyll) in different depths and allow for the analysis of the temporal development of stratification and O_2 concentration at the location of observation.

Greenwood et al. (2010) published the first data from continuous measurements of bottom oxygen concentration for two sites (North Dogger and Oyster Grounds) in a European shelf sea. From these measurements the dynamic interaction between stratification and the development towards low bottom O_2 concentration can be observed, as well as the rapid recovery to saturated O_2 conditions after the breakdown of stratification due to mixing in autumn.

Queste et al. (2013) presented an approach to extend the findings by Greenwood et al. (2010) to a spatial scale using data from a survey in August 2010, and ICES historical data. They found that the summer O_2 depletion near the Dogger Bank is not a recent phenomenon, however, its severity may have changed during the years. Their study showed, that in 2010 the largest part of the O_2 depletion zone was located in the central North Sea at about 57° N. They furthermore pointed out that it was likely caused

BGD
12, 12543–12610, 2015

by enhanced primary production in combination with the isolation of the deeper layers due to stratification and topographic features. Nevertheless, the question remains why this low O_2 concentration occur in regions of less intense stratification compared to the northern North Sea.

As stated by Greenwood et al. (2010), the data provided insight into the processes affecting the O_2 dynamics but it will require models to further elucidate the significance of the seasonal drivers. Ecosystem models provide insight into the balance between the physical and biological factors and processes governing the development of the bottom O_2 concentration. Thus, they can help to understand and interpret measurements of O_2 and related parameters and can further describe the history of events of low O_2 conditions.

In this study we use the three-dimensional physical-biogeochemical model system HAMSOM-ECOHAM5 to fill the gap between assessment requirements and data availability. The model provides temporally and spatially resolved information for the North Sea ecosystem allowing for the identification and characterisation of the key factors determining the inter-annual dynamics of the sub-thermocline and bottom O_2 concentration in different regions of the North Sea. For this purpose, we first validate the simulated bottom O_2 concentration with respect to its temporal development and spatial distribution in order to show that the model used captures the main features. Consequently, we present a regional characteristic of the parameters controlling the bottom O_2 dynamics and finally analyse the governing processes in terms of inter-annual and regional variations in their individual contribution to the O_2 development.

2 Material and methods

2.1 The ECOHAM model

Our study is based on the coupled physical-biogeochemical model system HAMSOM-ECOHAM5. The physical model HAMSOM (HAMburg Shelf Ocean Model; Backhaus,

BGD
12, 12543–12610, 2015

1985) is a baroclinic primitive equation model with a free surface and uses the hydrostatic and Boussinesq approximation (Pohlmann, 1991). HAMSOM is defined with a finite difference approach on an Arakawa C-grid (Arakawa and Lamb, 1977) using z coordinates. It is used to provide the temperature (T) and salinity (S) distribution, in addition to the fields for advective flow and the vertical turbulent mixing coefficient, used as forcing for the biogeochemical model ECOHAM5 (ECOsystem model HAMburg, version 5). An additional horizontal turbulent diffusion is not applied as Lenhart and Pohlmann (1997) found, that the applied advection scheme (component upstream) causes an already high numerical diffusion. For a detailed description of HAMSOM the reader is referred to Pohlmann (1991), further information on the application of HAMSOM can be found in Backhaus and Hainbucher (1987) and Pohlmann (1996).

The biogeochemical model ECOHAM5 is the successor of ECOHAM4 (Lorkowski et al., 2012; Pätsch and Kühn, 2008) and represents the pelagic and benthic cycles of carbon (C), nitrogen (N), phosphorus (P), silicon (Si) and O_2. As an extension to the classical NPZD (nutrients-phytoplankton-zooplankton-detritus) models, a representation of the "microbial loop" (Azam et al., 1983) is implemented using one functional group of bacteria. The model comprises the following state variables: 4 nutrients (nitrate, ammonium, phosphate, silicate), 2 functional groups of phytoplankton (diatoms, flagellates) and zooplankton (micro- and mesozooplankton), slowly and fast sinking detritus, labile and semi-labile dissolved organic matter (DOM), bacteria, dissolved inorganic carbon (DIC), total alkalinity and O_2. Furthermore, a module for the equilibrium chemistry of inorganic C is implemented allowing for the calculation of the air-sea flux of CO_2. The C : N : P ratios for phytoplankton, zooplankton and bacteria are fixed, but were chosen individually for each group (Lorkowski et al., 2012). The C : N : P ratios for detritus and DOM can evolve freely. Pelagic primary production is parametrised following Steele (1962) and light availability is limited by light attenuation of water, planktonic self-shading and suspended particulate matter (SPM).

The O_2 module within the ECOHAM5 model incorporates physical and biogeochemical processes determining the pelagic O_2 concentration (Pätsch and Kühn, 2008).

BGD
12, 12543–12610, 2015

The air-sea exchange of O_2 at the sea surface constitutes an important physical factor besides the effects of advective transport and vertical diffusion in the interior water column. The air-sea flux of O_2 in the present application is parametrised according to Wanninkhof (1992).

In relation to the biology, the O_2 cycle is linked to the C cycle by photosynthesis, zooplankton respiration and bacterial remineralisation. While photosynthesis is a source of O_2, the latter ones work as O_2 sinks. A further sink of O_2 is nitrification, the bacterial transformation of ammonium to nitrate. By this process, which is light-dependent, the O_2 cycle is linked to the N cycle within ECOHAM5. Nitrification only occurs under aerobic conditions (i.e. O_2 concentration > 0), which is a realistic constrain for the pelagic North Sea environment. Pelagic denitrification is implemented, but is negligible as it only occurs under anaerobic conditions. Pelagic anaerobic ammonium oxidation (anammox) is not implemented, however, can be neglected for the same reason. Except for primary production, the biological processes involved in the O_2 cycle are not temperature-dependent in the present model setup.

For the representation of the benthic remineralisation processes a simple sediment module is used. A layer of zero extent is defined below the last pelagic layer of each water column. There the deposited organic matter is collected and remineralised (Pätsch and Kühn, 2008). The benthic remineralisation of the organic matter is defined as a first-order process with relatively high remineralisation rates inhibiting year-to-year accumulation of deposited matter. The released dissolved inorganic matter is returned directly into the pelagic bottom layer. Different remineralisation rates are applied to organic C, N, P and Si (opal), resulting in different delays for the release into the pelagic. In ECOHAM5, the O_2 cycle (Pätsch and Kühn, 2008) is affected by the benthic remineralisation in a direct and indirect way. First, the remineralisation in the sediment is accompanied by the direct reduction of the O_2 concentration in the pelagic bottom layer above. Second, inorganic nitrogen is released from the sediment in form of ammonium, which can be nitrified within the water column under O_2 consumption. Nitrification is light-dependent, being stronger under low light conditions. According to Seitzinger and

BGD
12, 12543–12610, 2015

Giblin (1996), who suggested a tight coupling between benthic nitrification and denitrification, benthic denitrification depends on the benthic O_2 consumption in our model. Direct benthic nitrification and benthic anammox had to be neglected as the sediment has zero vertical extent (Pätsch and Kühn, 2008).

For a full set of the differential equations and parameter settings of ECOHAM5, including the different elemental ratios, the reader is referred to Lorkowski et al. (2012). Values of O_2 saturation concentration presented during the course of this study were calculated according to Benson and Krause (1984) using simulated T and S.

2.1.1 Model setup and external data

The model domain extends from 15.25° W to 14.083° E and from 47.583 to 63.983° N and comprises the whole North Sea, large parts of the northwestern European continental shelf (NECS) and parts of the adjacent northeastern Atlantic. The horizontal resolution is 1/5° with 82 grid points in latitudinal direction and 1/3° with 88 grid points in longitudinal direction. The horizontal grid of the model domain is shown in Fig. 2. The vertical dimension with a maximum depth of 4000 m is resolved by 31 z-layers with a surface layer of 10 m and thicknesses successively increasing with depth from 5 up to 1000 m in the layers below. The vertical has as resolution of 5 m between 10 and 50 m depth, which is relevant for the calculation of the MLD (Sect. 2.2. The described grid is applied to both models, HAMSOM and ECOHAM5.

The model system was run over the period 1977 to 2012. HAMSOM was initialised with a monthly-averaged climatology based on the World Ocean Atlas data set (WOA; Conkright et al., 2002). The meteorological forcing was calculated from NCEP/NCAR reanalysis data (Kalnay et al., 1996; Kistler et al., 2001) and provides 6 hourly information for air temperature, cloud coverage, relative humidity, wind speed and direction. The data were interpolated into the model grid and time step according to O'Driscoll et al. (2013) and Chen et al. (2014). Daily freshwater run-off data for 249 rivers were provided by Cefas and represent an updated dataset of that used by Lenhart et al.

BGD
12, 12543–12610, 2015

(2010) covering the whole simulation period. The same dataset encompassed nutrient loads used for the ECOHAM5.

At open boundaries, surface elevation was prescribed as a fixed (Dirichlet) open boundary condition (OBC) according to the M2 tide, while for horizontal transport velocities radiation OBCs were applied. For tracers (T and S) radiation and radiative-nudging OBCs were used in the case of inflow and outflow, respectively. A detailed description of the OBCs is provided by Chen et al. (2013). The HAMSOM simulation was carried out with a 10 min time step.

ECOHAM5 was run off-line with a time step of 30 min using the daily averages of the hydrographic and hydrodynamic fields generated by HAMSOM. In the model setup used, short wave radiation is attributed to the first layer (surface) only and the specific effect of light attenuation due to SPM and planktonic self-shading on the thermal structure is not taken into account. This approach is similar to the case of very large concentrations of shading material. In a sensitivity run we allowed light to penetrate into deeper layers accounting for light attenuation by water, SPM and phytoplankton. On average, the thermal structure during April–September 2002 (year of highest primary productivity) showed a minor decrease in the T difference between surface and bottom (-0.12 ± 0.10 K) and in the stratification period (-2 ± 5.6 days). The maximum decrease in average summer T difference was less than 0.5 K and confined to only a small area in the eastern central North Sea. The average effect of phytoplankton shading amounted to about 5 %.

For the biogeochemical state variables a climatology of depth-dependent monthly averages was prescribed at the boundaries, solely for DIC yearly changing data were provided (Lorkowski et al., 2012). To include the effect of SPM on the light climate, a daily climatology from Heath et al. (2002) was used covering the whole model domain. Data for atmospheric N deposition were compiled using a hybrid approach. This was required since the overall simulation period (1977–2012) exceeds the period of data available from the EMEP (Cooperative program for monitoring and evaluation of the long-range transmissions of air pollutants in Europe) model (1995–2012). First, the

BGD
12, 12543–12610, 2015

EMEP results for total deposition of oxidised (NO_x) and reduced nitrogen (NH_3) were interpolated to the model grid. Second, we calculated the average annual deposition rates for the NO_x and NH_3 for each grid cell, based on EMEP data for the period 1995–2012. The resulting spatially resolved arrays of average deposition rates were subsequently normalised by the spatial average of the whole domain to yield the spatially resolved anomaly fields. Finally, gridded deposition rates for individual years were obtained using (1) the gridded anomaly fields, (2) EMEP's spatially averaged (over our model domain) deposition rates for year 2005, and (3) long-term trends (normalised with respect to year 2005) for the temporal development of European emissions of NO_x and NH_3 (Schöpp et al., 2003, Fig. 2). The output of the biogeochemical simulation was stored as daily values (cumulative fluxes, state variable snapshots) for the whole domain and simulation period.

2.2 Extracting stratification parameters from model results

Stratification constitutes the prerequisite for the potential development of low O_2 conditions in the North Sea, and is defined by its (1) duration and (2) mixed layer depth (MLD). Therefore, these two parameters are crucial for the analysis of the O_2 dynamics conducted during the course of this study. As observations do not cover the whole model domain and simulation period it is inevitable to determine the duration of stratification and the MLD from the simulation results. For this purpose we developed a simple 2-step algorithm. First, the stratified period is determined using a temperature difference criterion:

$$S_{\text{strat}}(x,y,t) = \begin{cases} 1 & \Delta T|_{-H}^{0}(x,y,t) \geq 0.05\,\text{K} \\ 0 & \text{otherwise} \end{cases} \quad (1)$$

S_{strat} is a switch defining if a water column at location (x,y) and time t is stratified ($S_{\text{strat}} = 1$) or not ($S_{\text{strat}} = 0$) depending on the temperature difference ΔT between the surface and bottom depth H. The critical temperature difference $\Delta T_{\text{crit}} = 0.05\,\text{K}$ was determined by evaluating different ΔT_{crit} against the temporal development of simulated

BGD
12, 12543–12610, 2015

bottom O_2 at different locations within the model domain. For this purpose, we assumed that even if the surface mixed layer is interrupted due to mixing, this must not necessarily cause a complete overturning of the water column. Thus, even a minor difference in T indicates a bottom layer unaffected from vertical mixing. In addition, periods of stratified conditions are only considered as such, if they last for at least 5 days without any interruption. Otherwise bottom waters are considered to be ventilated again.

In the second step, in the case of stratification the MLD is defined as the depth D where the vertical temperature gradient $\delta T/\delta z$ has its maximum:

$$\mathrm{MLD}(x,y,t) = \begin{cases} D(\max(\delta T/\delta z)) & S_{\mathrm{strat}}(x,y,t) = 1 \\ 0 & \text{otherwise} \end{cases} \quad (2)$$

In addition, the discrete model grid implies the definition of the MLD as the bottom depth of the upper of the two layers between which the maximum gradient $\Delta T/\Delta z$ between the centre points of two vertically adjoining grid cells occurs.

2.3 Validation data

For the validation of the model results we used observation data from different sources. The datasets can be subdivided into two types: (1) temporally resolved, localised data and (2) spatially resolved "snapshots". The first type was used for the validation of the temporal development of O_2, whereas the second type was used to validate the general spatial patterns of bottom O_2 during late summer.

2.3.1 Localised, temporally resolved data – Cefas-SmartBuoy and MARNET

The problem of comparing sporadic O_2 measurements with simulated bottom O_2 concentrations was clearly shown by Lenhart et al. (2010, Fig. 9a). They compared bottom O_2 concentrations simulated by three different models against in-situ observations at the Dutch monitoring station Terschelling 135. Their first approach to directly compare observations and simulations of a single year revealed significant differences between

BGD
12, 12543–12610, 2015

simulated and observed bottom O_2 concentrations, with even lower simulated values falling below 6 mg L^{-1} in late summer. However, due to the sparse data, they could not determine whether these low simulated concentrations represented reasonable results for the corresponding period or not. Consequently, monthly averages and standard deviations of a 15 year dataset had to be used to unveil if O_2 concentrations below 6 mg L^{-1} were within a realistic range during the specific period at the location considered. In our study we use more or less continuous time series of bottom O_2 concentrations for the stations Cefas North Dogger and MARNET Ems to overcome this uncertainty in the validation.

Cefas operates a number of autonomous monitoring systems to provide up-to-date reports on marine water quality. One of these so-called "SmartBuoy" moorings is located directly north of the Dogger Bank at 55°41′ N, 2°16.80′ E (see Fig. 2, region 2). The SmartBuoy at this station (hereafter "North Dogger") was operational from 24 February 2007, to 15 September 2008 (Greenwood et al., 2010). At this site the water depth is 85 m and the measuring devices were located in 1, 31 and 85 m depth. T, S and O_2 concentrations were continuously recorded in the different depths. The O_2 concentrations were measured in a burst of between 5 to 10 min using an Aanderaa optode (AADI, Norway) with a frequency of 5 Hz (accuracy of 0.5 %). A 0–100 % calibration was conducted annually on each optode and results were corrected for drift using O_2 concentrations determined from discrete water samples. These samples were collected and preserved in triplicate according to Winkler, and subsequently analysed on board using an automatic titration system (Sensoren Instrumente Systeme, Germany). For a more detailed description of the data acquisition at North Dogger the reader is referred to Greenwood et al. (2010). For validation purposes the O_2 concentration data derived from the sensor at 85 m depth were used.

The BSH operates 12 marine monitoring stations within the MARNET programme. This programme focuses on the continuous monitoring of physical properties of seawater (T, conductivity, O_2 concentration and saturation) and hydrodynamic parameters, such as current velocities or sea level, to detect changes in the marine climate and to

BGD
12, 12543–12610, 2015

provide information model applications, e.g. storm surge forecast. At each MARNET station, the O_2 saturation is measured hourly in the surface and in the bottom layer using opto-chemical sensors (optodes).

At station Ems (54°10′ N, 6°21′ E; see Fig. 2, region 1), which has a bottom depth of 33 m, the two sensors are located at 6 and 30 m depth, respectively. The applied sensors have a resolution of 0.03 mg L^{-1} and an accuracy better than 0.26 mg L^{-1}. Before deploying the sensors a 0–100 % calibration is conducted, and they are re-calibrated after operation to quantify any drift. In addition, a regular on-site validation takes place using a calibrated fast optode (accuracy of ± 2 %) or by applying the Winkler titration (accuracy better than ± 1 %).

2.3.2 Spatially resolved "snapshot" data – the North Sea programme

During the North Sea programme, carried out by the Royal Netherlands Institute for Sea Research (NIOZ) with support from the Dutch Science Foundation (NWO) and the European Union, the North Sea was sampled from 18 August to 13 September 2001, and from 17 August to 5 September 2005 and 2008. The North Sea was covered by an approximate 1° × 1° grid, sampling approximately 90 stations in each of the three years. The station grid was denser in the Southern Bight, which is strongly affected by the major continental freshwater run-offs and to a lesser extent by the Baltic outflow. The station grid was coarser in the more homogeneous central and northern North Sea (Bozec et al., 2005, 2006; Salt et al., 2013). During each cruise, a total of 750 water samples was collected for dissolved O_2. In 2001, the O_2 concentration was determined by the Winkler titration using a potentiometric end-point determination with an accuracy of ± 2 µmol kg^{-1} (less than ± 0.07 mg L^{-1} depending on T and S). In 2005 and 2008, the O_2 concentration was obtained applying the spectrophotometric Winkler approach with a precision of less than 0.03 mg L^{-1}. A detailed description of the measurement system used is given in Reinthaler et al. (2006).

The data available were gridded to the model grid (Fig. 2). In the case of multiple measurements for the same model grid cell and date, the average of these measure-

BGD
12, 12543–12610, 2015

ments was used for validation. To compare our model results to these data, we calculated the averages and standard deviations of our simulation over the observation period of the corresponding year.

3 Results and discussion

3.1 Evaluation of the stratification and MLD criterion

For the present study, the stratification period and MLD constitute the major parameters defining the integration period and water volume used for the analysis of physical and biological drivers of the North Sea O_2 dynamics. As seasonal stratification in the North Sea is mainly T-driven (Burt et al., 2014), we used the simulated T to derive these information according to Eqs. (1) and (2), respectively. The applied critical T difference ($\Delta T_{crit} = 0.05$ K) differs significantly from common MLD criteria (e.g Kara et al., 2000, Table 1), thus, its evaluation is required.

For this purpose, Fig. 3 shows a Hovmöller diagram of simulated T at station North Dogger (see Fig. 2, region 2) for the year 2007, including the MLD (dashed magenta line) derived from the T field. Regarding the onset of stratification in late March it is shown, that the near-surface T (down to 25 m) starts to increase relatively to the T in deeper layers. The beginning of the stratified period on 26 April coincides very well with this slowly developing separation of surface and bottom waters. The maximum vertical T gradient at the onset occurs in 25 m depth. From that moment stratification according to Eq. (1) persists until 31 October, which may represent a slight overestimation as the maximum T gradient is found in 60 m depth already, indicating deep mixing.

During the course of the stratified period we can see that in the first 2 months (April/May) the MLD shows stronger fluctuations in terms of its actual depth. This is caused by the fact, that near-surface stratification is still relatively weak, and thus, short-term events of mainly wind-induced mixing can still reach depths of 35 m. These events are indicated by the episodic increase and decrease of surface T. From early

BGD
12, 12543–12610, 2015

June to end of July, the MLD is less variable in depth due to the persistent surface heating and less strong wind events. In late June a short-term decrease in surface T indicating enhanced mixing occurs which also results in a deepening of the MLD. From August until the end of the stratified period the MLD shows a deepening trend which is caused by the decreasing surface heating and increasing wind activity. However, in late August a shallowing of the MLD occurs which is related to an increase in the surface T.

In general, the criterion applied for the determination of the stratified period and MLD represents the stratification conditions quite well. However, it should be noted the criterion applied for the determination of the stratified period (Eq. (1)) may slightly overestimate the end of stratification. In addition, in regions with a less pronounced onset of stratification, i.e. a less distinct increase in surface T, the determined timing of the onset may be slightly too early. The use of the maximum T gradient to determine the MLD under stratified conditions yields reasonable results, and is closely related to real conditions as the thermocline is defined as the layer with the maximum T gradient.

3.2 Model validation

The validation of the model results using local time series data (Sect. 3.2.1) and spatially resolved snapshot data (Sect. 3.2.2) shows that the HAMSOM-ECOHAM5 model system represents the main features of bottom O_2 development in the North Sea. A detailed analysis of the validation results is given in the following.

3.2.1 Temporal development of bottom O_2

Figure 4 shows the comparison of simulated bottom O_2 against time series data at the Cefas station North Dogger for the years 2007 (a) and 2008 (b) and the MARNET station Ems during 2010 (c) and 2011 (d). The indicated stratification period was derived from the simulated temperature fields using Eq. (1).

BGD
12, 12543–12610, 2015

At North Dogger, observed and simulated bottom O_2 concentration show a steady decrease beginning with the onset of the stratification. While the stratification according to Eq. (1) starts a bit earlier compared to that described by (Greenwood et al., 2010), the beginning of the decrease in bottom O_2 concentration coincides well. The good agreement in the O_2 concentration at this point in time also shows that the spring T distribution is reproduced well as this value reflects mainly the saturation concentration.

Some small-scale fluctuations in the observations like the small minimum in the O_2 concentration at 15 April 2007, are not fully reproduced by the simulation. However, the general development is represented well by the model. The average reduction rate in the simulation is slightly lower compared to the observations which can be seen in the difference between the concentrations at beginning and end of the stratified period. The decrease in the O_2 concentration in 2007 suddenly ends with a mixing event between 10 and 12 November. It is shown, that stratification ends a bit earlier in the simulation, with the result that simulated bottom O_2 starts to recover while the observed concentration continues to decline until the mixing event, reaching an O_2 minimum of 6.4 mg L^{-1}. The observed O_2 concentration at the end of the stratified period is about 6.8 mg L^{-1}, while the simulation results in about 7.4 mg L^{-1}.

Unfortunately, the critical period in the development towards the minimum O_2 concentration is not covered in 2008, as the measurement ceased on the 14 September 2008. Nevertheless, we can see a similar slight overestimation of simulated O_2 concentration, but to a lesser degree compared to 2007. This is again due to a faster rate of reduction in the observations. In addition, some minor fluctuations can be seen in the observations, which are not represented by the model. However, as in 2007 the general trend of bottom O_2 is represented well by the simulation. It should be noted, that at station North Dogger, the centre depth of the model bottom layer is equal to 76 m (bottom depth of 82 m), while the sampling was conducted in 85 m depth. This difference may also affect the difference between simulated and observed O_2 concentrations.

The consistent slight overestimation of simulated bottom O_2 compared to the observation is likely to result from a consistent overestimation of summer bottom T, and thus

BGD
12, 12543–12610, 2015

vertical mixing, by the physical model HAMSOM (not shown). Nevertheless, keeping in mind the limited horizontal resolution of the model, the comparison to the observations at North Dogger is promising at it shows that the model is capable of reproducing the main features of seasonal bottom O_2 development as well as its inter-annual variability.

At MARNET station Ems the observed bottom O_2 concentration shows significantly larger intra-seasonal fluctuations than at Cefas station North Dogger. This applies to both years 2010 (panel c) and 2011 (panel d), and mainly results from the lower bottom depth, i.e. sampling depth (sensor in 30 m). The water column of the model at this location encompasses 6 vertical layers and is 35 m deep with a centre depth of the deepest grid cell of 32.5 m. In 2010, stratification starts to develop in late March, however, breaks down again and finally forms in late April lasting until mid-August.

The onset of O_2 reduction in the observations is in good agreement with the beginning of the decrease in the simulated O_2 concentration. From late May to late June, the observed bottom O_2 reveals a steep decrease which is not fully represented in the simulation, but shows the remarkable drop in observed O_2 in the second half of June, even though to a lesser extent. The same applies to the subsequent increase in observed bottom O_2 in early July, which is less distinct in the simulation. The replenishment of bottom O_2 in both, simulation and observation, occurs at a similar point in time, even though a bit earlier in the observations. This indicates, that the timing of the final breakdown of stratification is in good agreement. However, it has to be noted that the model tends to overestimate bottom O_2 in 2010, revealing a maximum difference of about 1 mg L^{-1}. The minor differences at the beginning and end of the year, representing mainly the saturation concentration, show that the general physical setting provided by the model is reasonable, even though some features during the summer period are not fully represented.

In contrast to 2010, continuous stratified periods derived from the simulation do not exceed 2 months at station Ems in 2011. This is also present in the *T* observation (not shown). Consequently, the temporal development of bottom O_2 represents mainly the temporal development of the O_2 saturation concentration. The large fluctuations of up

BGD
12, 12543–12610, 2015

to ± 2 mg L^{-1} visible in the observations indicate the presence of different water masses as station Ems is episodically influenced by the coastal freshwater signal. In addition, the tides may have an effect on the short-term. These events are not represented in the simulation due to the low spatial resolution and the daily output time step of the simulation. Besides these short-term changes the difference between simulated and observed bottom O_2 concentration are less than 0.8 mg L^{-1} with higher summer values in the simulation.

The differences between simulated and observed O_2 concentration at the beginning and end of the year are less than during the summer period staying below ± 0.4 mg L^{-1}. This and the relatively good agreement in the temporal development of bottom O_2 during the stratified period show that the general features of bottom O_2 at station Ems in 2011 are captured by the model.

3.2.2 Spatial distribution of late summer bottom O_2

The profile data collected within the North Sea programme during late summer 2001, 2005 and 2008 provide a highly valuable dataset as they reveal spatial patterns in the North Sea O_2 distribution as well as inter-annual variations within this region. Figure 5 shows the spatial distribution of the average simulated and observed O_2 concentrations in the model bottom layer for the years 2001 (panel a), 2005 (panel b) and 2008 (panel c), and the standard deviation related to the averages in 2005 (panel d). The averaging period for the simulations corresponds to the complete observation period for each year, listed in the bottom right corner of each panel.

Comparing the simulated and gridded observed bottom O_2 concentrations for all three years it is shown that the simulation tends to overestimate the bottom O_2 concentration in most areas, however, the general spatial and inter-annual variations visible in the observations are represented well by the model. In 2001, the observations show the lowest concentration of all years with minimum values of 5.9 mg L^{-1} in the area 54–57° N, 4.5–7° E. This minimum is similarly present in the model results with values

BGD
12, 12543–12610, 2015

slightly below 7 mg L^{-1}. Considering the maximum concentrations in the North Sea, the observations yield values of 9.3 mg L^{-1} off the southern tip of Norway and values between 8.7 to 8.8 mg L^{-1} in the deepest parts of the Norwegian Trench. The very high observed value at the northwesternmost sampling site represents an outlier due to the decreasing vertical resolution of the model in greater depth.

The comparison of the differences between 2005 and 2001 with respect to the 2001 minimum area shows that the observed minimum values are about 0.3 mg L^{-1} higher in 2005 than in 2001. This relative increase compared to 2001 is reproduced well by the simulation showing a similar increase by about 0.2 mg L^{-1} in this area in 2005. The observations show lowest bottom O_2 a bit north and south of the simulated minimum, but still relatively low values less than 7.2 mg L^{-1} in the centre of the simulated minimum. Highest observed values are located in the very deep area at the eastern end of the Norwegian Trench, and in the inner German Bight yielding an O_2 concentration of 9.3 mg L^{-1}. The model indicates only slightly higher values in the German Bight area compared to 2001, due to the low grid resolution. In the northern North Sea, the simulation shows lower values compared to 2001, which can be seen in the observations as well.

In 2008, the observations reveal significantly higher bottom O_2 concentrations in the area of the 2001 minimum, compared to the previous years. In contrast, observed concentrations in most other parts of the North Sea are lower than in 2001 and 2005. The overall minimum concentration in 2008 of 7.2 mg L^{-1} is reached close to the Dutch coast. Analysing the simulated bottom O_2 with respect to this inter-annual change in the spatial pattern, we can see that simulated bottom O_2 also yields lower values in the southern North Sea, and significantly higher values in the 2001 minimum area. For the western central and northern North Sea the picture is different. Here, the observations result in consistently lower values compared to 2001 and 2005, whereas the simulated O_2 shows higher values in most areas, except for the eastern Norwegian Trench.

In general, the basin-wide distributions of simulated bottom O_2 represent the spatial patterns shown in the observations quite well, even though absolute values are not

BGD
12, 12543–12610, 2015

always reflected. Both observed and simulated bottom O_2 concentrations show that the 50 m-isobath (broadly along 54° N, 0° E to 57° N, 8° E; Thomas et al., 2005) marks the separation line between the northern regions unaffected of low O_2 conditions and the southeastern parts, which are more vulnerable to low O_2 concentrations. In addition, the model demonstrated to be capable of capturing inter-annual variations in the bottom O_2 development. In combination with the results of the temporally resolved validation (Sect. 3.2.1), this confirms, that the described model setup provides reliable information on the internal physical and biological processes driving the O_2 dynamics in the North Sea.

As the comparison of the simulated bottom O_2 concentration with the observed ones showed that our model is able to reproduce the main features of late summer O_2 concentrations, the standard deviation of the simulation during the observation period gives useful insight in the temporal variability of O_2 during a period of 3 to 4 weeks in late summer. Figure 5d shows the standard deviation of the simulation and observation for 2005. The picture given for the simulation in this year is mainly representative for the years 2001 and 2005 as well. It shows that in most areas of the North Sea the changes in bottom O_2 during August/September are very low throughout a period of 3 to 4 weeks, indicated by a standard deviation of less than 0.1 mg L^{-1}. This in turn implies that measurements taken around this period can be considered as representative for late summer conditions. In addition, the small standard deviations for the simulation confirm that using the average over a period of up to 4 weeks provides a reasonable measure for most areas. This implies that observations taken in late summer before the breakdown of stratification represent a synoptic picture of the late summer bottom O_2 conditions.

However, the validation presented in Sect. 3.2.1 showed that in some areas lowest concentrations of bottom O_2 may occur remarkably later in the year (see Fig. 4a). Consequently, the picture obtained from observations taken in August/September does not necessarily reflect the spatial distribution of minimum bottom O_2 concentrations. In addition, two areas east and west of the 2001 minimum region reveal higher variability

BGD
12, 12543–12610, 2015

during the sampling period indicated by a standard deviation of up to 0.45 mg L^{-1}. In the western one, stratification may break down earlier in the year due to the combined effect of lower water depth and the onset of autumn storms, resulting in enhanced mixing. This underlines the importance of choosing the appropriate point in time to conduct measurements with respect to the monitoring of low O_2 conditions.

The small standard deviation of the observations, which is a result of the data gridding, shows that in most regions vertical O_2 gradients near the bottom are negligible. However, at the southeastern edge of the Dogger Bank and northwest of Denmark, high values of 0.75 and 0.59 mg L^{-1}, respectively, show that low O_2 conditions (compare low average values at the corresponding locations in Fig. 5b) can occur in a relatively thin layer above the bottom.

3.2.3 A quantitative assessment of the model performance

The Taylor diagram (Fig. 6; Taylor, 2001) provides a quantitative assessment of the model performance with respect to simulated bottom O_2 concentrations in relation to the validation data used in Sect. 3.2.1 and Sect. 3.2.2: (a) station Cefas North Dogger (see Fig. 4a and b) station MARNET Ems (see Fig. 4c and d) the spatially resolved data (see Fig. 5a–c). For this purpose, we merged the observations and corresponding simulation data of the different years into one continuous series of data for each of the three datasets. The Taylor diagram presents the correlation coefficients (COR), standard deviations (STD) and centred root-mean-square differences (RMSD) of the simulation relative to the observation. The two latter values are normalised by the STD of the corresponding observations.

The correlation coefficient COR between observation X and simulation Y is calculated as follows for each of the three datasets:

$$\mathrm{COR}(X,Y) = \frac{1}{N \cdot \mathrm{STD}(X) \cdot \mathrm{STD}(Y)} \cdot \sum_{i=1}^{N} (X_i - \overline{X})(Y_i - \overline{Y}). \quad (3)$$

BGD
12, 12543–12610, 2015

Here, N equals the number of observation-simulation pairs. The index i indicates a single value of the considered dataset, while $\overline{X}$ and $\overline{Y}$ represent the average values. The unnormalised STD of a dataset Z (observation or simulation) is calculated as:

$$\mathrm{STD}(Z) = \sqrt{\frac{1}{N} \cdot \sum_{i=1}^{N} \left(Z_i - \overline{Z}\right)^2}. \quad (4)$$

The unnormalised RMSD between observation X and simulation Y is calculated as:

$$\mathrm{RMSD}(X,Y) = \sqrt{\frac{1}{N} \cdot \sum_{i=1}^{N} \left[(X_i - \overline{X}) - (Y_i - \overline{Y})\right]^2}. \quad (5)$$

The statistics for the time series data confirm the good agreement between simulation and observation shown in Fig. 4. For both stations, COR is high with values of about 0.95 and the normalised RMSD is less than 0.38. The RMSD values are mainly due to the larger range and higher (seasonal and sub-seasonal) variability in the observed bottom O_2, which is also indicated by the normalised STDs of about 0.73 and 0.82 for Cefas North Dogger and MARNET Ems, respectively. For the spatially resolved data, COR reaches only about 0.64. This lower correlation was also shown in Fig. 5 by the inter-annual variations in the simulations and observations between year 2008 and the previous years, when the simulation revealed a relative change inverse to that in the observations in the northern North Sea. The normalised RMSD is about twice as high as for the time series resulting in 0.77, which can be attributed to the greater regional differences in the observed bottom O_2 concentration with higher maximum and lower minimum values. The normalised STD equals 0.67 which also indicates the less strong spatial differences in the simulation. These statistics confirm the picture given by Fig. 5, which showed that the spatial patterns in the observed bottom O_2 concentration are basically reproduced by the model, with only slight shortcomings with respect to the

BGD
12, 12543–12610, 2015

amplitude of the bottom O_2 concentration and inter-annual variations in some regions of the North Sea.

In summary, the validation based on time series and spatially resolved observations showed that our model system is capable of reproducing the main temporal (seasonal and inter-annual) and spatial features of bottom O_2 in the North Sea. Hence, the analysis of the O_2 dynamics based on HAMSOM-ECOHAM5 will provide valuable insight in temporal and spatial variations of the North Sea O_2 dynamics.

3.3 Simulated stratification periods and minimum bottom O_2

In Fig. 7a and b the longest continuous stratification period after Eq. (1) derived from simulated T is presented for the years 2002 (a) and 2010 (b). Both years show similar stratification patterns which are in good agreement with the different stratification regimes described by Pingree et al. (1978) and van Leeuwen et al. (2015). The resulting stratification periods of > 180 days for large parts of the central and northern North Sea are in good agreement with van Leeuwen et al. (2015). They applied a density-based stratification criterion on model results to subdivide the North Sea into areas of different stratification characteristics, and showed that most areas of the seasonally stratified central and northern North Sea reveal stratification periods of 170 to 230 days.

Comparing the corresponding minimum concentration of bottom O_2 (Fig. 7c and d) the simulation results show significant differences which one would not expect when only comparing the duration of stratification. The minimum bottom O_2 concentration in 2002 in the region from 55–56.5° N, 4.5–7.5° E constitutes the lowest O_2 concentration during the whole period 2000–2012 reaching values of below 5.8 mg L^{-1}. In contrast, the duration of stratification in this area is similar or even longer in 2010 than in 2002. The O_2 concentrations in 2002 are even below the O_2 threshold applied by OSPAR (6 mg L^{-1}; OSPAR-Commission, 2005) and persist for about one month (not presented). In contrast, 2010 represents a year with relatively high minimum bottom O_2 concentrations being above 7.3 mg L^{-1} in the whole model domain.

BGD
12, 12543–12610, 2015

The areas directly north and south of the Doggerbank also reveal lowered bottom O_2 concentrations in both years. This increased potential for low O_2 conditions north and south of the Doggerbank is in good agreement with observed bottom O_2 time series in these regions (Greenwood et al., 2010). Queste et al. (2013) also observed lower bottom O_2 concentrations north of the Dogger Bank in August 2010, however, they found the minimum concentrations a bit further north around 57° N.

The discrepancy between minimum O_2 concentration in the two years compared to the quite similar stratification patterns demonstrates that stratification is an important prerequisite for low O_2 conditions, but other factors control the actual O_2 development. This poses the question which physical and biological processes drive the O_2 dynamics in the North Sea during the summer stratified period. Based on the processes driving O_2 depletion, our primary hypothesis is that the production and aggregation of organic matter within the mixed layer, subsequently sinking and being remineralised below the thermocline, is the main cause for low O_2 conditions in the deeper layer.

3.4 An O_2-related characteristic of the North Sea

Besides stratification, eutrophication is considered as a major driver for developing low O_2 conditions (e.g. Diaz and Rosenberg, 2008; Kemp et al., 2009). This implies that biogeochemical factors play an important role for the near-bottom O_2 development in general, not only for O_2 depletion. Increased primary production within the mixed layer and the resulting enhanced organic matter export into the layers below the MLD represent the main source for degradable organic matter in the deeper layers. Therefore, these quantities must be considered when characterising different regions of the North Sea with respect to O_2. In addition, organic matter can be advected from surrounding waters in the form of phyto- or zooplankton and detritus, subsequently sinking out of the mixed layer.

Another important criterion is the water volume below the thermocline (Druon et al., 2004). A smaller volume separated from the surface due to stratification holds a lower initial inventory of O_2 than a larger volume even though concentrations are similar or

BGD
12, 12543–12610, 2015

even higher in the smaller volume. Thus, our set of O_2-related characteristics consists of: mixed layer primary production (PP_{mld}), horizontal advection of organic matter into and out of the mixed layer ($ADH_{org,in}$ and $ADH_{org,out}$; including phyto-/zooplankton and detritus), organic matter export below the MLD (EXP_{org}; only detritus), mixing of O_2 below the thermocline (MIX_{O_2}) and the sub-MLD volume V_{sub}.

To detect regional characteristics within the North Sea area, we defined 4 different sub-domains encompassing 4×4 model water columns each (see Fig. 2, red boxes): (A) southern North Sea (SNS) under strong tidal influence, (B) southern central North Sea (SCNS) with high inter-annual variability in stratification, (C) northern central North Sea (NCNS) with a dominant summer stratification each year, and (D) northern North Sea (NNS) with a dominant summer stratification each year and a strong influence of the Atlantic. For all these regions, the parameters described above were calculated for the years 2000–2012 relative to a reference depth D_{ref}, which is defined as the bottom depth of the model layer directly below the annual maximum MLD among all four regions. We decided to use a D_{ref} >MLD to ensure that for the different regions all parameters were determined on a comparable level. This is especially important for MIX_{O_2}, as the vertical O_2 gradient may show significant differences depending on whether it is determined between the two layers above and below the thermocline, or between two layers both below the MLD. This implies that the values for PP_{mld}, $ADH_{org,in}$ and $ADH_{org,out}$ are integrated from the surface to D_{ref}, whereas EXP_{org} and MIX_{O_2} are the temporally integrated vertical fluxes through D_{ref}. The same D_{ref} was applied to all regions, but inter-annual variations were allowed.

To determine the annual maximum MLD, we first calculated the stratification period for the 4×4-regions B–D using Eq. (1). Region A was excluded from this calculation as no persistent MLD developed due to tidal mixing. In this context, $S_{strat}(t)$ of a region is only 1 if $S_{strat}(x,y,t) = 1$ for all 16 water columns within a 4×4-region. The daily MLD for each water column within a region was calculated by applying $S_{strat}(t)$ to Eq. (2), and subsequently the daily MLD of the region is defined as the median of these 16 daily values. The annual MLD for each region was then determined as the median of

BGD
12, 12543–12610, 2015

this daily time series. Finally, the annual maximum MLD among all 4 regions is used to receive the reference depth D_{ref}.

Table 1 shows the averages over the period 2000–2012 of the above described critical quantities for all four regions (A–D). The annual values were calculated relative to a D_{ref} of 25 m which corresponds with the bottom depth of the layer below the maximum MLD for each year and region according to Eqs. (1) and (2). In 2005 and 2007, D_{ref} was reset to this depth, as the actual D_{ref} was equal to the minimum bottom depth of region A, not allowing for the calculation of all parameters. The different quantities are compared for two different integration periods: the whole year and 1 April to 30 September (hereafter "summer").

The mixed layer net primary production, PP_{mld}, is strongest in the coastal region A and shows decreasing values towards the central North Sea. On an annual basis the SCNS region B has a level of about 92 % compared to the productive coastal region A. The corresponding value for the NCNS region C and NNS region D is about 80 %, respectively. The small differences between annual and summer PP_{mld} are related to the fact that most of the production takes place from April to September.

Despite the high PP_{mld} at the coast, Table 1 shows the strongest contribution of gross advection of organic matter, $ADH_{org,in}$ and $ADH_{org,out}$, for the SCNS region B. This feature would not be visible by looking only at net advection, since the difference in the net fluxes is again largest for region A. Both regions show positive net advection, while the two northern regions C and D are characterised by a negative advective net flux, i.e. loss of organic matter due to advective transport. Regions C and D are located north of the Dogger Bank, which means they are within the recirculation system of the northern Atlantic inflow. In this region, net advection results in a loss in organic matter as the recirculated northward flowing water has higher concentrations of organic matter than the incoming Atlantic water. Interestingly, the model reveals the highest ADH_{org} for region B even exceeding ADH_{org} in the highly productive region A which is also affected by the strong continental coastal current.

BGD
12, 12543–12610, 2015

The vertical export of organic matter EXP_{org} below D_{ref} is clearly linked to the production of organic matter, PP_{mld}. Region B obtains an EXP_{org} of 75 % of that in the coastal region A, which corresponds with a higher net advective organic matter import of 6.7 g C m^{-2} in region A compared to only 1.6 g C m^{-2} part in Region B. EXP_{org} in region C reaches only about 65 % relative to region A. For region D the annual and summer values reach about 77 % of the corresponding values in the coastal region A. In contrast, the export of organic matter during summer is relatively stable at about 83 % of the annual values for all regions, which is related to the fact that the major part of primary production occurs during the stratified period.

The vertical mixing of O_2, MIX_{O_2}, is highest within the coastal region A because the tidal mixing inhibits the development of a seasonal thermocline. How persistent the O_2 ventilation works throughout the year is nicely illustrated by the fact that the value for the 6 month period is nearly half the annual value. It is interesting to note that the annual values for the vertical mixing in the two northern regions C and D are higher than the one for the SCNS region B. However, the dramatic impact of the occurrence of a strong seasonal thermocline is clearly shown in the reduction of the vertical mixing fluxes to about 7 % in the two northern regions and to about 36 % in region B relative to the annual values. As stratification in region B lasts shorter than in region C and does not cover the whole period from April to September, the impact on the vertical O_2 flux for region B is overestimated. When taking into account only the period when all regions – except region A – are stratified, the flux reduces to about 17 % of the annual flux.

The O_2 concentration at the beginning of the year reveals minor differences between the regions with a range of 8.9–9.3 mg L^{-1}. Comparing these values to those at the beginning of April, it can be seen that the O_2 concentration is continuously increasing during the first three months of the year reaching values between 9.5 and 10.1 mg L^{-1}. This increase is caused mainly by decreasing T resulting in a higher O_2 solubility, i.e. higher saturation concentration $O_{2,sat}$. However, all considered regions show an increase in the actual O_2 concentration higher than that in $O_{2,sat}$, ranging between about

BGD
12, 12543–12610, 2015

14 % higher values in region B and 33 % higher values in region A. This suggests that the onset primary production during this early period causes the additional increase in the O_2 concentration on a North Sea wide scale.

In order to give an impression of the impact of the organic matter export EXP_{org} on the O_2 dynamics of the water volume below the MLD V_{sub}, we link the amount of exported organic matter to the amount of O_2 available within V_{sub} assuming the organic matter is remineralised to its full amount in the area of settlement. Based on the O_2 concentration at the beginning of April, the total amount of O_2 results in 1365 kt for region B and 4590 kt for region C. The total amount of exported organic matter is calculated as the product of EXP_{org} and the total area of the considered region. This calculation yields 130 kt C and 115 kt C for the regions B and C, respectively. As O_2 consumption and C release occur with a molar ratio of 1 : 1 during bacterial remineralisation (Neumann, 2000), the equivalent of total mass of O_2 in kt O_2 can be calculated by using the molar masses of C (12.0107 g mol^{-1}) and O_2 (2 × 15.994 g mol^{-1}). Finally, we receive the daily O_2 consumption in kt O_2 d^{-1} by dividing by the total duration of the considered 6 months-period (= 183 days). Division of the initial mass of O_2 by this daily rate provides an estimate of the amount of time required for the consumption of the entire amount of O_2 available in the volume below the MLD. This calculation yields a period of 719 days for region B, whereas the corresponding value for region C is significantly higher with 4348 days.

If we base this calculation on the threshold of 6 mg O_2 L^{-1} used by OSPAR (OSPAR-Commission, 2005), the results for the two regions diverge even more yielding 283 and 4270 days for region B and C, respectively. As EXP_{org} shows only minor spatial variability between the two regions, these great differences in the resulting consumption illustrate clearly the large influence of the volume below the MLD, V_{sub}, on the temporal development of the O_2 concentration.

BGD
12, 12543–12610, 2015

3.5 Driving mechanisms and inter-annual variability of sub-thermocline O_2 dynamics

As shown in Fig. 7, similar stratification periods in different years do not necessarily lead to similar distributions of bottom O_2. This suggests that stratification constitutes a mandatory condition for low O_2 conditions, but inter-annual variations in other physical and biological factors determine whether the sub-thermocline O_2 conditions fall below a critical level or not.

We calculated O_2 mass balances for the years 2002 and 2010 for region 3, encompassing 2×2 model grid cells (see Fig. 2), to analyse the different dynamics below the thermocline (hereafter "sub-MLD") resulting in the significant inter-annual variations of the minimum bottom O_2 concentration. This region shows the lowest bottom O_2 concentration in the North Sea during most simulated years and is located a bit west of the absolute O_2 minimum in 2002 (see Fig. 7c). This was done to show how inter-annual variations in the sub-MLD processes affect the the sub-MLD O_2 which also controls the O_2 development in the bottom layer. The annual median MLD was determined analogous to that for the 4×4-regions as described in Sect. 3.4.

The sub-MLD O_2 mass balances for 2002 and 2010 are presented in Fig. 8a and b, respectively. The shown actual O_2 concentration and saturation concentration represent the average values within the analysed volume. The fluxes presented are cumulative changes in the O_2 concentration of the considered volume, i.e., the values at the end of the stratified period reflect the total net change of the O_2 concentration due to the corresponding physical or biological process. Positive and negative values at the end of the stratification period indicate net gain and loss, respectively. The slope of each line represents the intensity of the corresponding flux at the specific moment in time, i.e. a steep positive (negative) slope implies a strong gain (loss) effect.

We analyse the inter-annual variations between the different processes affecting sub-MLD O_2 in relation to the setting defined by stratification in 2002 and 2010. The algorithm for the calculation of the median MLD, which defines the upper limit of the anal-

BGD
12, 12543–12610, 2015

ysed volume, resulted in 15 m for both years. Consequently, the volume considered is identical with about 60.7 km^3. The stratification period lasts 187 days in both years. The only difference with respect to stratification period and MLD is the timing of the onset and breakdown of stratification. In 2010 stratification already starts on 11 March whereas in 2002 the onset occurs 20 days later.

The comparison of the sub-MLD O_2 concentrations (solid magenta) at the beginning of the stratified period shows that the concentration of 9.81 $mg\,L^{-1}$ in 2002 is about 0.33 $mg\,L^{-1}$ lower than in 2010. The concentrations at the end of stratification also are lower in 2002 reaching about 7.13 $mg\,L^{-1}$. The corresponding value in 2010 is about 0.64 $mg\,L^{-1}$ higher. Accordingly, the net decrease in O_2 during the stratified period is more than 0.31 $mg\,L^{-1}$ higher in 2002 than in 2010.

The diverging temporal development of the simulated O_2 concentration and the corresponding saturation concentration $O_{2,sat}$ (dash-dotted magenta) reveals that the decrease in O_2 is caused not only by decreasing O_2 solubility. This implies that other physical and/or biological factors must play an important role for the O_2 development below the MLD. In, addition, the only minor differences in $O_{2,sat}$ at the beginning of the stratified period between 2002 and 2010 reveal, that differences in O_2 solubility only have a minor effect on inter-annual variations in this region and instead are caused by variations in other physical and biological factors affecting O_2.

3.5.1 The influence of advection and mixing

The comparison of advection (ADV_{O_2}; including horizontal and vertical components; dashed blue line) and vertical mixing (MIX_{O_2}; turbulent diffusion; dashed dark blue) for the years 2002 and 2010 shows strong annual and inter-annual variations. ADV_{O_2} regularly changes its influence on the sub-MLD O_2 concentration during stratification in both years. However, comparing the temporally integrated effect, ADV_{O_2} causes a net gain of about 0.83 $mg\,L^{-1}$ in 2002, whereas in 2010 it results in a net loss of about −0.21 $mg\,L^{-1}$. Interestingly, advection positively affects the O_2 concentration during the

BGD
12, 12543–12610, 2015

last 2–3 weeks of the stratified period in both years. In 2002, this strong increase is accompanied by a slight net increase in the O_2 concentration and even precedes the recovery of the O_2 concentration due to enhanced vertical mixing. This suggests that advective input of oxygenated water from surrounding regions can play an important role for the recovery of the sub-MLD O_2 concentration especially in the later phase of the stratified period.

The vertical mixing through the mixed layer MIX_{O_2} in 2002 has a positive effect on the O_2 concentration throughout the whole stratified period adding up to a total gain in O_2 concentration of almost $1.6\,mg\,L^{-1}$. In late April and late June two events of strong downward mixing occur causing a rapid gross increase in the O_2 concentration. In the latter case, MIX_{O_2} is even strong enough to trigger a net increase in the O_2 concentration. This mixing event coincides with a decrease of $O_{2,sat}$ by $-0.05\,mg\,L^{-1}\,d^{-1}$ on 1 July which represents the strongest decrease in $O_{2,sat}$ during the whole year.

In 2010, MIX_{O_2} also provides a net gain in O_2 integrated over time, but is about $0.65\,mg\,L^{-1}$ lower than in 2002. During the first 3 weeks of stratification, MIX_{O_2} shows a remarkably stronger positive effect on O_2 than in 2002, which suggests that in this phase the thermocline is not yet fully developed and still allows for enhanced vertical mixing. However, after this period MIX_{O_2} weakens and finally has almost no net effect on the sub-MLD O_2 concentration from end of April until late September. During this phase the vertical mixing even causes temporary declines in O_2, e.g. in mid-June, which result from the fact that highest O_2 concentrations do not occur directly at the surface, but around the MLD. The lower O_2 concentrations directly at the surface result from the higher T, and thus, lowered O_2 solubility. Consequently, events of wind-induced MLD deepening can bring warmer, less oxygenated water from the uppermost layer into the colder deeper layers causing these slight reductions in the sub-MLD O_2 concentration.

With respect to ADV_{O_2} the sub-MLD mass balances reveal that the net effect of advection on the O_2 concentration in region 3 is quite different between the years. In

BGD
12, 12543–12610, 2015

2002, ADV_{O_2} causes a net increase of O_2 about half as important as the vertical mixing, whereas in 2010 advection causes a net decrease of the O_2 concentration.

To obtain information on the inter-annual variabilities in the changes in O_2 concentration due to advection and vertical mixing during the whole period 2000–2012 we compare the standard deviation (STD) of these physical factors with respect to the cumulated affect during the stratified period. In addition, the comparison of the effect in 2002 and 2010 to the corresponding averages helps to classify these two years in relation to the effect of the physics. As the duration of stratification varies between the different years within this period we calculate the annual average daily rates of change in O_2 due to these factors by dividing their integrated effect during the stratified period by the duration of stratification in the corresponding year. By this we obtain a comparable measure independent of the duration of stratification during the different years.

The average values for the whole period 2000–2012 result in $0.0005 \pm 0.0017\,mg\,L^{-1}\,d^{-1}$ for ADV_{O_2} and $0.0081 \pm 0.0034\,mg\,L^{-1}\,d^{-1}$ for MIX_{O_2}. The small positive value for ADV_{O_2} shows that on average, advection is only a minor source of O_2. However, the large relative STD of 327 % in ADV_{O_2} indicates the large inter-annual variability during the analysed period. This implies that advection can provide both, a remarkable gain or loss, during different years. The average and STD for MIX_{O_2} show that vertical mixing causes an increase in sub-MLD O_2 in most years.

3.5.2 Biological drivers of the sub-thermocline O_2 dynamics

The comparison of the effects of advection and vertical mixing showed that in 2002 both factors provide favourable conditions for uncritical sub-MLD O_2 concentrations, whereas in 2010 the integrated effect of advection and mixing is less beneficial for the O2 concentration, even though it is still positive. However, it has to be kept in mind, that MIX_{O_2} is mainly driven by the vertical gradient in the O_2 concentration and higher biological consumption below the MLD would result in a stronger MIX_{O_2} under similar stratification conditions. The significantly lower simulated minimum O_2 concentration in

BGD
12, 12543–12610, 2015

2002 compared to 2010 emphasises the great importance of the biological processes for the sub-MLD O_2 development.

In contrast to the integrated effect of the physical factors, it is shown that the integrated effect of the biological processes causes a net loss in O_2. The only source process for O_2 is primary production (PP; dashed light blue) which causes a gross increase in O_2 of about 1.06 mg L^{-1} in both years. The analysis of the biological sink processes reveals that the pelagic remineralisation of organic matter (REM_{pel}; dashed light green) has the strongest effect on the sub-MLD O_2, exceeding even the integrated effect of benthic remineralisation (REM_{sed}; dashed yellow), zooplankton respiration (RES_{zoo}; dashed dark green) and nitrification (NIT; dashed red). Among the last-mentioned processes RES_{zoo} has the strongest effect on the O_2 concentration and NIT is least affecting O_2. This a consistent picture throughout the whole period 2000–2012. However, the individual fluxes show remarkable inter-annual variations, especially comparing the two years presented.

In 2002, REM_{pel} is strongest among all years 2000–2012 causing an O_2 consumption of about −3.08 mg L^{-1}. In contrast, 2010 represents the year with the second lowest REM_{pel} being about 0.72 mg L^{-1} less than in 2002. In terms of RES_{zoo} the difference between the two years is also large with a 2010 value of 0.74 mg L^{-1} which is 0.60 mg L^{-1} less than in 2002 (77 % of the 2002 value). For RES_{zoo}, the 2002 value also constitutes the highest among all years, while the 2010 value marks the lowest value. In 2002, REM_{sed} is again the highest value of the whole period 2000–2012 with about −1.18 mg L^{-1} O_2 reduction, while the consumption in 2010 represents the second lowest value and is 0.46 mg L^{-1} less than in 2002 (55 % of the 2002 value). NIT is also strongest in 2002 with an integrated change in the O_2 concentration by about −0.56 mg L^{-1}. In terms of NIT, 2010 also shows values about 12 % below the average value of -0.40 ± 0.08 mg L^{-1}, and is 0.21 mg L^{-1} lower than the 2002 value. In terms of REM_{sed} and NIT, the 2010 values account for only about 61 and 62 % of the 2002 values, respectively. This similarity shows the link between these two processes. NIT

BGD
12, 12543–12610, 2015

is light-limited being higher under low light conditions, thus it mainly occurs in deeper layers where REM_{sed} constitutes the major source for ammonium.

The integrated effect of all biological sink processes (REM_{pel}, REM_{sed}, RES_{zoo} and NIT) adds up to $-6.16\,mg\,L^{-1}$ in 2002, and a $2\,mg\,L^{-1}$ lower value in 2010, i.e. the total biological O_2 consumption in 2002 is almost 1.5 times higher than in 2010 and 1.2 times higher than the average value of $-5.10 \pm 0.63\,mg\,L^{-1}$ of the period 2000–2012. Interestingly, the relative contribution of the individual processes to the overall biological O_2 consumption shows only minor inter-annual variations during the analysed period. REM_{pel} has an average relative contribution of 53.3 ± 1.8 %, while REM_{sed} accounts for 17.3 ± 1.1 %. For RES_{zoo} and NIT the average relative contributions result in 21.6 ± 1.6 % and 7.7 ± 1.0 %, respectively.

According to our primary hypothesis the amount of organic matter which is produced in the upper layers and subsequently sinks into the sub-MLD zone must be significantly higher in 2002 than in 2010. The comparison of the summer PP within the upper 25 m (not presented; calculation analogous to Table 1) reveals a 1.3 times higher value in 2002. The export of organic matter below this depth is nearly 1.6 times larger than in 2010. As zooplankton is not considered in this comparison, the mismatch between the factors for PP and EXP_{org} is likely to result from higher zooplankton growth, i.e. organic matter production, which is also indicated by the 81 % higher zooplankton respiration in 2002 compared to 2010 (see Fig. 8a and b). The good agreement between the differences in EXP_{org} and the integrated effect of the biological O_2 sinks confirms that the supply of detrital matter to the deep layers is the driving force of sub-MLD O_2 consumption. In this context, it should be noted that 2002 represented an exceptional year in terms of especially high riverine input of organic matter and nutrients into the North Sea (Lenhart et al., 2010). Thus, the increased nutrient availability is likely to be the main cause for the low O_2 conditions during this year.

Besides the differences in the temporally integrated effect of the individual biological processes between 2002 and 2010, Fig. 8a and b reveal some differences in their development during the stratified period. In 2002, the mixing events in late April and

BGD
12, 12543–12610, 2015

late June show direct and indirect effects on the biological processes. The mixing-induced renewal of the nutrient pool causes short-term increases in PP around the MLD. Consequently, the reduction due to RES_{zoo} and REM_{pel} is enhanced. In addition, the mixing causes increased EXP_{org} which also triggers stronger REM_{pel}. The change in the O_2 concentration during these events shows that only the stronger event in late June causes a net increase in O_2, whereas O_2 continuously decreases during the weaker event in late April. This suggests that only sufficiently strong mixing results in a positive net effect on O_2, while during events of less strong mixing, biological consumption can balance or even exceed the combined positive effect of ventilation and increased PP.

3.6 Bottom layer dynamics of the North Sea O_2 minimum zone

The analysis of the different physical and biological processes contributing to the development of sub-MLD O_2 concentration unravels the complexity behind the different processes affecting the formation of a low O_2 zone. However, as lowest O_2 concentrations usually occur in the bottom layer it is important to know which processes are the main contributors to the O_2 dynamics in this layer. For this purpose, Fig. 8c and d show the mass balances for the bottom layer of region 3 for 2002 and 2010. The bottom layer in this region encompasses a volume of about 14.4 km^{-3} which accounts for less than 24 % of the total sub-MLD volume (V_{sub}).

Comparing the O_2 concentration in the bottom layer at the beginning of the stratified period to that in V_{sub}, we see only slightly lower values in the bottom O_2 concentrations for both years, yielding 9.79 and 10.12 $mg\,L^{-1}$ for 2002 and 2010, respectively. This constitutes a relative difference between bottom O_2 concentration and sub-MLD concentration of less than 0.2 % for both years. These small differences match our expectations, as the water column is considered to be well-mixed before the onset of stratification. In contrast, the difference in the bottom O_2 concentration at the end of stratification between the bottom layer and V_{sub} is worth mentioning. In 2002, the bot-

BGD
12, 12543–12610, 2015

tom O_2 concentration results in 6.76 mg L^{-1} being 0.37 mg L^{-1} lower than in V_{sub}. In 2010, the bottom O_2 concentration yields 7.55 mg L^{-1} which is 0.22 mg L^{-1} lower compared to V_{sub}. That means, bottom O_2 reduction in 2002 is about 13 % faster than in V_{sub}, and still about 10 % faster in 2010.

The analysis of the effect of the physical factors, ADV_{O_2} and MIX_{O_2}, on the bottom O_2 concentration provides a different picture compared to V_{sub}. While in 2002 ADV_{O_2} shows a similar effect on O_2 as for the sub-MLD O_2 with a contribution of about 75 % relative to the contribution to sub-MLD O_2, its effect in 2010 is opposite to that for V_{sub}. However, its integrated effect in 2010 is only slightly positive with a value of about 0.1 mg L^{-1} on the bottom O_2 concentration. During the last 3 weeks of stratification in 2002, the same positive effect of ADV_{O_2} as in the sub-MLD mass balance is shown, initiating the recovery of the bottom O_2 before MIX_{O_2} intensifies at the end of the stratified period. This underlines that the gain in O_2 due to advection can balance or even exceed the still ongoing consumption in the final phase of stratification.

With respect to MIX_{O_2} the mass balances also reveal differences between the bottom layer and V_{sub}. In 2002, the effect on the bottom O_2 increased compared to its influence on the sub-MLD O_2 by factor 3.6. In 2010, we see a similar increase by factor 3.4, and different to its effect on the sub-MLD O_2, MIX_{O_2} is continuously increasing the bottom O_2 concentration during the whole stratified period. The significant gain in the integrated effect of MIX_{O_2} as well as the consistent picture given for both years results from the fact that the bottom layer shows generally lower O_2 than the layer directly above due to benthic remineralisation. This persistent gradient drives the downward diffusion of O_2 into the bottom layer.

Considering the relative contribution of the biological processes consuming O_2 in the bottom layer the picture also changed compared to that for sub-MLD O_2: as shown for the years 2002 and 2010, the comparison of the average value of 2000–2012 reveals that the bottom layer REM_{sed} accounts for 50.1 ± 1.2 % of the total biological O_2 consumption which represents the largest contribution, while REM_{pel} contributes to 32.2 ± 1.4 %. This reveals that aerobic remineralisation consistently adds up to more

BGD
12, 12543–12610, 2015

than 80 % of the biological O_2 consumption in the bottom layer. The shift in the relative contribution between these two processes occurs due to the fact that in ECOHAM5 REM_{sed} only has a direct effect on the deepest pelagic layer. That means, the absolute change in mass of O_2 due to REM_{sed} is identical in both cases, while the change in concentration differs in relation to the different volumes considered.

To demonstrate the effect of REM_{sed} on bottom O_2, we calculated the total changes in mass of O_2 due to REM_{pel}, and due to the REM_{sed} and REM_{pel} for V_{sub} and the bottom layer and finally calculate the ratio of their effect on V_{sub} to that on the bottom layer. The total change in O_2 mass is calculated by multiplying the changes in the O_2 concentration with the corresponding volumes for the period 2000–2012 (not including 2008 due to shallower mixed layer). This yields that the total change in mass in V_{sub} due to REM_{pel} is about 4.7 ± 0.1 times larger than in the bottom layer. In contrast, the change in mass due to the combined effect of REM_{pel} and REM_{sed} is only about 2.4 ± 0.1 times larger for V_{sub}. In addition, the ratio between V_{sub} and the bottom layer volume is equivalent to about 4.2. This shows that REM_{pel} is less efficient in the bottom layer than in the other parts of V_{sub} and emphasises the great importance of REM_{sed} for the dynamics of bottom O_2.

Regarding the rate of O_2 consumption due to benthic remineralisation, our model yields values between 3.9 and 6.5 $mmol\,m^{-2}\,d^{-1}$ for region 3. These values are in the same order as those derived from observations giving a range from 7 to 25 $mmol\,m^{-2}\,d^{-1}$ for a nearby station (Upton et al., 1993, station 3), however, rather at the lower end of this range. This suggests, that our model may slightly underestimate benthic remineralisation resulting in higher bottom O_2 concentrations compared to observed values.

As shown in Fig. 8 the influence of RES_{zoo} on the bottom O_2 concentration is lower than in V_{sub} as zooplankton tends to stay in the upper part of the water column where phytoplankton concentrations are higher. Its relative contribution accounts for only 11.3 ± 1.2 % during the years 2000–2012. NIT represents the weakest sink for bottom O_2 with an average contribution of 6.4 ± 0.6 % during these years. The standard devi-

BGD
12, 12543–12610, 2015

ations for RES_{zoo} and NIT are relatively high compared to their average contribution indicating higher inter-annual variations.

The analysis of the processes in the bottom layer clearly shows that benthic aerobic remineralisation constitutes the major driver for the development of low O_2 conditions in the North Sea O_2 minimum zone. Pelagic aerobic remineralisation still has a significant effect on bottom O_2, but accounts for a remarkably lower proportion than in the whole sub-MLD volume. This large impact of the two remineralisation processes is in good agreement with the common picture of bacterial respiration being the driving process for low O_2 conditions under stratified conditions (e.g. Diaz and Rosenberg, 2008). In addition, the comparison of the sub-MLD and bottom layer mass balances for the two years showed that the processes in the pelagic zone, especially pelagic remineralisation, are crucial for the bottom O_2 concentrations as they define the potential O_2 supply into the bottom layer. In combination with the inter-annual differences in surface PP presented and the subsequent enhanced export of organic matter in 2002, this confirms that sufficiently long stratification provides the basis for low O_2 conditions, but the biological processes constitute the key element for the development of O_2 depletion.

3.7 Spatial variability in the North Sea bottom O_2 dynamics

In order to unveil the regional differences in North Sea O_2 dynamics, Fig. 9 shows the mass balances for the sub-MLD volume of two regions in the southern (panel a) and northern North Sea (panel b) in 2002 (see Fig. 2 for location of regions 4 and 5) in comparison to that for region 3 (Fig. 8a).

Regarding the stratification characteristics, region 4 and 5 show some differences compared to region 3. Even though the MLD according to Eqs. (1) and (2) also results in 15 m for both regions, the stratification periods differ. In region 4, the period between the first and last day of stratification accounts for only 163 days compared to 187 in region 3. Additionally, stratification is temporarily intermittent in late April and early July. In region 5, stratification lasts for 211 days without any interruptions. Considering

BGD
12, 12543–12610, 2015

the onset of stratification, stratification in region 4 and 5 starts 3 days and 1 day earlier than in region 3, respectively.

For a better understanding of the different effects of physical and biological factors in the different regions, it has to be kept in mind that the water depths and bottom layer volumes differ between the three regions. Region 3 has an average water depth of 47.75 m and a bottom layer volume of about 14.4 km^3, while region 4 is characterised by an average depth of 45 m and a bottom layer volume of 11.9 km^3. The greatest difference occurs for the region 5, which has an average bottom depth of 99.25 m and a bottom layer volume of 16.3 km^3.

The temporal development of O_2 in the bottom layer shows some significant differences for both regions between the three regions. Besides the lower O_2 concentrations at the beginning of the stratified period in both regions (9.79, 9.74 and 9.46 $mg\,L^{-1}$ in region 3, 4 and 5, respectively), the concentrations at the end of stratification for both regions are higher than in region 3. These values reach 6.98 $mg\,L^{-1}$ in region 4 and 7.61 $mg\,L^{-1}$ in region 5, compared to 6.76 $mg\,L^{-1}$ in region 3.

In region 4, the temporary breakdown of stratification in early July causes a remarkable increase in sub-MLD O_2 due to enhanced mixing visible in the sudden increase of MIX_{O_2}. This increase even exceeds the biological consumption, and the bottom O_2 pool is fully replenished which is illustrated by the match between O_2 and $O_{2,sat}$. It should be noted, that the strongest increase in MIX_{O_2} precedes the interruption of stratification according to Eq. (1). This is caused by the fact that the complete overturning of the water column, and thus the vanishing of the surface-to-bottom T difference, requires more time than the breakdown of the near-surface thermocline. Integrated over the stratified period the effect of MIX_{O_2} is almost 1.5 times higher than in region 3. In region 5, MIX_{O_2} represents a significantly lower supply of O_2 accounting for only 16 and 11 % of that in region 3 and 4, respectively. This mainly relates to the significantly greater water depth resulting in more stable stratification as wind-induced mixing only affects the upper tens of metres. ADV_{O_2} has an opposite effect in regions 4 and 5 relative to region 3, however, showing only minor negative effects integrated over time.

BGD
12, 12543–12610, 2015

The comparison of the biological processes shows that as in region 3 the effect of bottom PP is negligible in region 4 and 5, due to light limitation. The integrated effect of the O_2 consuming processes reveals that among the three regions, consumption is largest in region 4 exceeding even that of region 3 by about 16 %. Biological O_2 consumption in region 5 accounts for only about 29 % of that in region 3. In that context, it is worth mentioning that the summer PP in the upper 25 m (calculation analogous to Table 1) in region 4 is similar to region 3, while the EXP_{org} below this depth is even 19 % higher than in region 3. The difference between EXP_{org} and PP can also be attributed to local zooplankton production. The good agreement in the relative differences of EXP_{org} and biological consumption between region 3 and 4 confirms the strong link between these two factors in shallower regions. In region 5, the upper layer PP and EXP_{org} account for only 78 and 62 % of that in region 3, respectively.

Interestingly, the relative contributions of the different sink processes in region 4 are in the same order as in region 3. REM_{sed} represents the largest contributor with about 54.6 % of the total biological consumption, while REM_{pel} accounts for 27.2 %. For RES_{zoo} and NIT the relative contributions result in 13.6 and 4.6 %, respectively. Consequently, the combined effect of REM_{sed} and REM_{pel} accounts for 81.8 % which is similar to region 3.

Comparing the rates of benthic remineralisation derived from the simulation to literature for region 4, which lies within the Oyster Grounds area, provides a similar picture as for region 3. The simulation yields a benthic remineralisation rate of about $8.9\,mmol\,m^{-2}\,d^{-1}$ for 2007, while observational studies near this site obtained rates between 5.6 and $30.6\,mmol\,m^{-2}\,d^{-1}$ (Lohse et al., 1996; Weston et al., 2008). This confirms the picture from region 3, that the model most likely underestimates the impact of benthic remineralisation on the bottom O_2. In addition, this higher rate in region 4 compared to region 3 underlines the high potential for low O_2 conditions in the Oyster Grounds under persistent seasonal stratification. This is in good agreement with the findings by Greenwood et al. (2010), who observed bottom O_2 concentrations less than $6\,mg\,L^{-1}$ in this area.

BGD
12, 12543–12610, 2015

The comparison of the relative contribution of REM_{pel} and REM_{sed} in region 5 reveals some changes with respect to these two processes. REM_{sed} accounts for about 70 % of the total biological O_2 consumption, while REM_{pel} contributes to only about 20 %. With respect to the volume and corresponding greater thickness of the bottom layer we would expect a lower relative contribution of REM_{sed} compared to the other regions. However, the generally lower amount of organic matter exported into the deeper layer (63 % of that in region 3) results in a lower concentration of pelagic bacteria. On the one hand, this causes lower O_2 consumption due to REM_{pel}, and on the other hand, enhances REM_{sed} relative to REM_{sed} as more organic matter is deposited and remineralised in the sediment.

Considering the combined effect of stratification, i.e. mixing, water depth and bottom layer volume, and biological consumption, it is shown, that the shorter duration of stratification and the occurrence of strong mixing in region 4 prohibit the development of low O_2 conditions, even though biological consumption is larger than in region 3. In region 5 stratification lasts longer than in the other two regions without any interruptions, however, the biological consumption is significantly lower than in region 3 and 4 as less organic matter is supplied to the deeper layers. In addition, the water depth, i.e., the sub-MLD volume, in region 5 is significantly larger than in the other regions. This suggests that region 5 is unlikely to be affected by low bottom O_2 concentrations. However, this region lies in the area where Queste et al. (2013) found a bottom O_2 minimum in 2010. They concluded that this O_2 minimum resulted from a combination of stratification, limiting the ventilation of the deeper layers with oxygenated surface waters, and the specific bathymetry, which limits the lateral exchange with the O_2-enriched surrounding waters. Our results showed that advection only has a minor influence on the bottom O_2 in this area, which indicates that other processes may have caused this O_2 minimum.

BGD
12, 12543–12610, 2015

3.8 Interpreting observed bottom O_2 at North Dogger

At station North Dogger (see Fig. 2, region 2) continuous bottom O_2 data were recorded in the years 2007 and 2008 (Greenwood et al., 2010). These observations shown in Fig. 4a and b showed similar O_2 concentrations of about 9.5 $mg\,L^{-1}$ at the beginning of the stratified period, but revealed a faster decrease in bottom O_2 during 2007 compared to 2008. As simulation also showed this tendency with respect to the inter-annual differences, we want to use the model-based O_2 mass balance to explain the differences in the observations between the two years at North Dogger. These mass balances for 2007 and 2008 are presented in Fig. 10a and b, respectively.

Calculating the average rates of O_2 during the stratified period we obtain about $-0.009\,mg\,L^{-1}\,d^{-1}$ for 2007. For 2008, the simulation yields a lower rate of about $-0.007\,mg\,L^{-1}\,d^{-1}$. The value for 2007 slightly underestimates the value of $-0.012\,mg\,L^{-1}\,d^{-1}$ derived from the observation by Greenwood et al. (2010), however, is still in the same order. Even though the temporal development in 2008 was not discussed in detail by Greenwood et al. (2010) as the data recording ended before minimum bottom O_2 was reached, the available data indicate lower reduction rates in 2008 compared to 2007 (see Fig. 4a and b).

This poses the question, which processes affecting O_2 vary between the two years. Regarding the O_2 supply due to the physical factors ADV_{O_2} and MIX_{O_2}, it is shown, that the integrated effect of both is quite similar for both years providing a gross increase in O_2 of about 1.35 $mg\,L^{-1}$ integrated over the stratified period. The only small temporally integrated effect of ADV_{O_2} shows that even though the North Dogger area is affected by relatively strong advection (Greenwood et al., 2010), this must not necessarily result in enhanced ventilation in terms of bottom O_2. This relates to the fact that the deeper waters in the surrounding regions show only slightly higher O_2 concentrations, which causes an only minor net effect of advection on bottom O_2. This demonstrates, that the main inter-annual variations are related to biological factors.

BGD
12, 12543–12610, 2015

While the two years show basically similar features in terms of the biological consumption processes, these processes are characterised by higher rates in 2007 than in 2008. In 2007, the integrated O_2 consumption of all biological sink processes results in $-3.4\,mg\,L^{-1}$, which corresponds with an average reduction rate of $-0.0154\,mg\,L^{-1}\,d^{-1}$. For 2008, the simulation yields a by $0.6\,mg\,L^{-1}$ lower integrated O_2 consumption related to a by $0.002\,mg\,L^{-1}\,d^{-1}$ lower reduction rate. This constitutes a relative difference of 13 % between the reduction rates due to biological consumption of the two years. Comparing the EXP_{org} below 25 m depth during summer (calculation analogous to Table 1), the same relative difference occurs, which again shows the strong link between organic matter export and biological O_2 consumption.

Despite the significant inter-annual differences in EXP_{org}, the relative contribution of the different processes to the overall bottom O_2 consumption shows only minor changes between the two years. In both years REM_{sed} accounts for about 58 %, while REM_{pel} accounts for about 31 %. RES_{zoo} and NIT contribute to about 3 and 8 % in both years, respectively. This shows that inter-annual variations in the O_2 dynamics at North Dogger are mainly driven by differences in the organic matter export. The steeper decrease in bottom O_2 in 2007 results from the enhanced supply of organic matter and the subsequent increased degradation by bacteria. The enhanced release of ammonium due to pelagic and benthic remineralisation consequently triggers an increase in nitrification.

The large contribution of bacterial remineralisation (REM_{sed} and REM_{pel}) accounting for almost 90 % of the overall biological consumption at station North Dogger confirms that the estimates for C remineralisation rates made by Greenwood et al. (2010) provide reasonable results. However, as NIT also accounts for about 8 % of the total biological consumption, this process should be considered to obtain more precise estimates for C remineralisation rates at Station North Dogger.

Our analysis of the observed temporal development of bottom O_2 at station North Dogger using the HAMSOM-ECOHAM5 model system showed, that despite minor differences between simulation and observation, ecosystem models can help to in-

BGD
12, 12543–12610, 2015

terpret measurements with respect to the underlying dynamics. Meire et al. (2013) undertook a similar study for the Oyster Grounds using a one-dimensional physical-biogeochemical model. However, in our study we showed that three-dimensional models can provide the combined benefit of data interpretation and the identification of spatial and temporal patterns in the O_2 dynamics.

4 Conclusions and perspectives

The North Sea is one of the shelf regions regularly suffering from seasonal hypoxia in the bottom water (Diaz and Rosenberg, 2008; Emeis et al., 2015; Rabalais et al., 2010). However, not all areas of the North Sea are similarly affected by low O_2 conditions (e.g. Queste et al., 2013) due to different characteristics with respect to stratification and upper layer productivity. Our study demonstrated that biogeochemical models can be useful to understand and explain these differences.

Our model-based analysis of different factors affecting O_2 (Sect. 3.4) showed that the North Sea can be subdivided into three different regimes in terms of O_2 dynamics: (1) a highly productive, non-stratified coastal regime (region A), (2) a productive, seasonally stratified regime with a small sub-thermocline volume (region B), and (3) a productive, seasonally stratified regime with a large sub-thermocline volume (regions C and D). While the regimes of type 1 and 3 are unlikely to be affected by low O_2 conditions due to either continuously ongoing ventilation (type 1) or the large sub-thermocline volume damping the effect of O_2 consumption (type 3), type 2 is highly susceptible to low O_2 conditions. This results from the specific combination of high upper layer productivity and small sub-thermocline volume, which causes a strong impact of the consumption processes on the decrease in the bottom O_2 concentration.

The model-derived O_2 mass balances showed that inter-annual variations in the sub-thermocline and in the bottom O_2 development are mainly caused by differences in the upper layer productivity as increased primary productivity directly and indirectly enhances the export of organic matter into the deeper layers. Higher primary produc-

BGD
12, 12543–12610, 2015

tion results in larger amounts of dead phytoplankton sinking below the thermocline, and increased phytoplankton growth enhances zooplankton growth which causes an additional increase in organic matter production and export. Furthermore, enhanced zooplankton growth increases O_2 consumption due to zooplankton respiration. The increased export of organic matter results in stronger bacterial remineralisation which in turn triggers nitrification due to the stronger release of ammonium.

With respect to the biological O_2 consumption our study revealed remarkable differences between the dynamics of the sub-thermocline volume and the bottom layer. While pelagic bacteria represent the major consumer in the sub-thermocline volume, benthic remineralisation constitutes the major driver for the bottom O_2 development. In addition, our results suggest that the relative contribution of the different O_2 consuming processes in the bottom layer at a certain location depends on the water column depth and is independent of the overall consumption. Benthic remineralisation consistently accounts for more than 50 % of the bottom O_2 consumption and revealed an increasing relative contribution with increasing bottom depth. In contrast, pelagic remineralisation is characterised by a decreasing influence in deeper regions, due to the fact, that organic matter concentrations within the pelagic bottom layer are lower in greater depth. Its relative contribution to the overall bottom O_2 consumption exceeds consistently 20 %. The effect of zooplankton respiration varies between almost no effect in deep regions and up to 14 % in shallower areas, whereas nitrification shows only minor variations in its relative contribution (3–8 %).

While our results showed that organic matter production and the subsequent bacterial remineralisation are the main drivers for the O_2 consumption, our study confirmed that vertical mixing represents the only efficient gain term for bottom O_2 in most regions. In addition, our simulations revealed that advection of O_2-enriched water from the surrounding areas may play an important role for the recovery of sub-thermocline and bottom O_2 concentrations at the end of the stratified period, even before stratification breaks down and vertical mixing replenishes the bottom O_2 concentration.

BGD
12, 12543–12610, 2015

With respect to the regional distribution of hypoxia in the North Sea, observations and model results revealed that the area between 54–57° N and 4.5–7° E shows the highest potential for hypoxic conditions, but also areas directly north and south of the Doggerbank experience lowered bottom O_2 concentrations.

By providing this valuable insight, the present study demonstrates the potential of ecosystem models to describe key features of the O_2 dynamics as an integral part of the North Sea ecosystem. Model simulations can unveil the complex interplay between hydrodynamical conditions and biological processes, and thus, can help to interpret the O_2 dynamics in the context of the natural variability of the ecosystem. This can be related to weather conditions which result in different stratification patterns of the North Sea, or in variations in the biological production. The latter can be induced by anthropogenic drivers, such as increased atmospheric deposition (Troost et al., 2013) or riverine nutrient input as shown for the exceptionally wet year 2002 (Lenhart et al., 2010). Thus, ecosystem models can help to estimate the impact of these anthropogenic impacts on the bottom O_2 depletion in offshore areas which are susceptible to hypoxia.

With the capability to describe the temporal development and spatial patterns of bottom O_2, ecosystem models can be used to obtain a more detailed picture of the spatial extent and duration of hypoxic conditions. This is useful for the detection of regions susceptible to low O_2 conditions which therefore require enhanced management. While this study focused on the general characterisation of the key factors driving the North Sea O_2 dynamics, detailed studies could, e.g., further investigate the cause-effect relationship between the high riverine nutrient loads and the major hypoxic event in 2002. In combination with the observational data available, this supports a meaningful discussion of the eutrophication status of the North Sea.

This assessment can be extended towards new measures to combat eutrophication within the Water Framework Directive (WFD), in which dissolved O_2 plays an important role as one of the five "General chemical and physiochemical elements supporting the biogeological elements" for assessment (Best et al., 2007). As the WFD assessment depends strongly on the description of pristine conditions related to natural nutrient

BGD
12, 12543–12610, 2015

levels (Topcu et al., 2009), ecosystem models can provide insight in the O_2 dynamics under these pristine conditions, and in addition, for the application of the WFD measures (Schernewski et al., 2015) on the North Sea. Even though the WFD regulation is applied only on narrow band along the coastline, the question of how nutrient reductions under WFD measures will effect the entire North Sea ecosystem, also in terms of bottom O_2 conditions, is highly relevant. Therefore, O_2 is one of the main descriptors under the Marine Framework Directive (MSFD) for the definition of the "Good environmental Status" as the target condition.

The article on the "spreading dead zones" by Diaz and Rosenberg (2008) resulted in an increased public awareness of the hypoxia issue, also in the context of the debate on climate change. One can start the discussion with the straight forward argument that climate change scenarios show an earlier onset and increased intensity of stratification for the North Sea due to increasing temperatures (Lowe et al., 2009; Meire et al., 2013). In addition, an increase in temperature will decrease the O_2 solubility in the bottom layer (Weston et al., 2008). Changes in the weather conditions, such as increased precipitation or other extreme events (Rabalais et al., 2010), could furthermore lead to increased nutrient loads triggering higher primary production which could increase the risk of hypoxia (Justić et al., 2003). In contrast, Gröger et al. (2013) predicted a North Sea wide reduction in primary production by about 30 % due to reduced winter nutrient import from the Atlantic. Another potential impact was argued by van der Molen et al. (2013), who concluded that the temperature-driven increase in metabolic rates and nutrient cycling will be followed by an increase in primary production. In combination with an increase in the benthic metabolic rates and other constrains, this will eventually lead to a decrease in the bottom O_2 concentration.

As these potential changes in the O_2 conditions will also affect the biological community in the North Sea (Emeis et al., 2015), it is important to foster the analysis of potential impacts of climate change and changes in nutrient loads on the O_2 dynamics. This study provided evidence that ecosystem models can contribute to the better understanding of the complex interplay of hydrodynamical and biogeochemical processes

BGD
12, 12543–12610, 2015

controlling the bottom O_2 dynamics in the North Sea. This study showed that ecosystem models can be used to either interpret in-situ O_2 measurements, or to estimate the impact of climate change or nutrient reduction scenarios with respect to hypoxia and its concomitants. Thus, they can provide relevant information for the ecological management of marine coastal ecosystems.

Data availability

The time series data from the Cefas SmartBuoy programme can be accessed via: http://cefasmapping.defra.gov.uk/Smartbuoy. The time series data of BSH MARNET programme can be accessed via: http://www.bsh.de/en/Marine_data/Observations/MARNET_monitoring_network/. The spatially resolved data from the North Sea cruises 2001, 2005 and 2008 have been released in the framework of the EU-FP6 project CARBOOCEAN and can be accessed via: http://dataportal.carboocean.org/.

Acknowledgements. We like to thank Sonja van Leeuwen from Cefas for providing updated data on freshwater and nutrient loads for the major rivers across Europe. We further thank Jerzy Bartnicki for providing atmospheric nitrogen deposition data from the European Monitoring and Evaluation Programme (EMEP). We also thank Dilek Topcu and Uwe Brockmann from the University of Hamburg for providing the map of observed North Sea hypoxia. The model simulation was conducted on Blizzard, the IBM Power6 mainframe at the German Climate Computing Centre (DKRZ) in Hamburg. The North Sea sampling in 2001, 2005 and 2008 was supported by the Dutch Science Foundation (NWO), CARBOOCEAN (EU-FP6) and the Royal Netherlands Institute for Sea Research (NIOZ). Markus Kreus was partly financially supported by the Cluster of Excellence "CliSAP" (EXC177), University of Hamburg, funded by the German Science Foundation (DFG). This study was supported by the German Environmental Protection Agency (UBA) in Dessau, in the frame of the project "Implementation of Descriptor 5 Eutrophication to the MSFD", SN: 3713225221.

BGD
12, 12543–12610, 2015

References

Arakawa, A. and Lamb, V.: Computational design of the basic dynamical processes of the UCLA general circulation model, Methods in Computational Physics, 17, 173–265, 1977. 12550

Azam, F., Fenchel, T., Field, J., Gray, J., Meyer-Reil, L., and Thingstad, F.: The ecological role of water-column microbes in the sea, Mar. Ecol.-Prog. Ser., 10, 257–263, doi:10.3354/meps010257, 1983. 12550

Backhaus, J.: A three-dimensional model for the simulation of shelf sea dynamics, Deutsche Hydrografische Zeitschrift, 38, 165–187, doi:10.1007/BF02328975, 1985. 12549

Backhaus, J. and Hainbucher, D.: A finite difference general circulation model for shelf seas and its application to low frequency variability on the North European Shelf, Elsev. Oceanogr. Serie, 45, 221–244, doi:10.1016/S0422-9894(08)70450-1, 1987. 12550

Benson, B. and Krause, D.: The concentration and isotopic fractionation of oxygen dissolved in freshwater and seawater in equilibrium with the atmosphere, Limnol. Oceanogr., 29, 620–632, doi:10.4319/lo.1984.29.3.0620, 1984. 12552

Best, M., Wither, A., and Coates, S.: Dissolved oxygen as a physico-chemical supporting element in the Water Framework Directive, Mar. Pollut. Bull., 55, 53–64, doi:10.1016/j.marpolbul.2006.08.037, 2007. 12590

Bozec, Y., Thomas, H., Elkalay, K., and de Baar, H.: The continental shelf pump for CO_2 in the North Sea – evidence from summer observation, Mar. Chem., 93, 131–147, doi:10.1016/j.marchem.2004.07.006, 2005. 12557

Bozec, Y., Thomas, H., Schiettecatte, L.-S., Borges, A., Elkalay, K., and de Baar, H.: Assessment of the processes controlling the seasonal variations of dissolved inorganic carbon in the North Sea, Limnol. Oceanogr., 51, 2746–2762, doi:10.4319/lo.2006.51.6.2746, 2006. 12557

Brockmann, U. and Eberlein, K.: River input of nutrients into the German Bight, in: The Role of Freshwater Outflow in Coastal Marine Ecosystems, Springer, Berlin Heidelberg, 231–240, available at: http://link.springer.com/chapter/10.1007/978-3-642-70886-2_15, accessed 29 June 2015, 1986. 12547

Brockmann, U. and Topcu, D.: Confidence rating for eutrophication assessments, Mar. Pollut. Bull., 82, 127–136, doi:10.1016/j.marpolbul.2014.03.007, 2014. 12548

Brockmann, U., Billen, G., and Gieskes, W.: North Sea nutrients and eutrophication, in: Pollution of the North Sea, Springer, Berlin Heidelberg, 348–389, available at: http://link.springer.com/chapter/10.1007/978-3-642-73709-1_20, accessed 29 June 2015 1988. 12547

BGD
12, 12543–12610, 2015

Brockmann, U., Laane, R., and Postma, J.: Cycling of nutrient elements in the North Sea, Neth. J. Sea Res., 26, 239–264, doi:10.1016/0077-7579(90)90092-U, 1990. 12547

Burt, W., Thomas, H., Pätsch, J., Omar, A., Schrum, C., Daewel, U., Brenner, H., and de Baar, H.: Radium isotopes as a tracer of sediment-water column exchange in the North Sea, Global Biogeochem. Cy., 28, 786–804, doi:10.1002/2014GB004825, 2014. 12546, 12547, 12558

Chen, X., Liu, C., O'Driscoll, K., Mayer, B., Su, J., and Pohlmann, T.: On the nudging terms at open boundaries in regional ocean models, Ocean Model., 66, 14–25, doi:10.1016/j.ocemod.2013.02.006, 2013. 12553

Chen, X., Dangendorf, S., Narayan, N., O'Driscoll, K., Tsimplis, M., Su, J., Mayer, B., and Pohlmann, T.: On sea level change in the North Sea influenced by the North Atlantic Oscillation: local and remote steric effects, Estuar. Coast. Shelf S., 151, 186–195, doi:10.1016/j.ecss.2014.10.009, 2014. 12552

Claussen, U., Zevenboom, W., Brockmann, U., Topcu, D., and Bot, P.: Assessment of the eutrophication status of transitional, coastal and marine waters within OSPAR, Hydrobiologia, 629, 49–58, doi:10.1007/s10750-009-9763-3, 2009. 12548

Conkright, M.E., Locarnini, R.A., Garcia, H.E., O'Brien, T.D., Boyer, T.P., Stephens, C., Antonov, J.I.: World Ocean Atlas 2001: objective analyses, data statistics and figures CD-ROM documentation, National Oceanographic Data Center Internal Report, National Oceanographic Data Center, Silver Spring, MD, 17, 2002. 12552

de Jong, F.: Marine Eutrophication in Perspective: On the Relevance of Ecology for Environmental Policy, Springer Science and Business Media, Berlin Heidelberg, 2006. 12547

Diaz, R. and Rosenberg, R.: Spreading dead zones and consequences for marine ecosystems, Science, 321, 926–929, doi:10.1126/science.1156401, 2008. 12546, 12568, 12582, 12588, 12591

Druon, J.-N., Schrimpf, W., Dobricic, S., and Stips, A.: Comparative assessment of large-scale marine eutrophication: North Sea area and Adriatic Sea as case studies, Mar. Ecol.-Prog. Ser., 272, 1–23, 2004. 12568

Ducrotoy, J., Elliott, M., and de Jonge, V.: The North Sea, Mar. Pollut. Bull., 41, 5–23, doi:10.1016/S0025-326X(00)00099-0, 2000. 12546

Emeis, K.-C., van Beusekom, J., Callies, U., Ebinghaus, R., Kannen, A., Kraus, G., Kröncke, I., Lenhart, L., Lorkowski, I., Matthias, V., Möllmann, C., Pätsch, J., Scharfe, M., Thomas, H.,

BGD
12, 12543–12610, 2015

Weisse, R., and Zorita, Z.: The North Sea – a shelf sea in the Anthropocene, J. Marine Syst., 141, 18–33, doi:10.1016/j.jmarsys.2014.03.012, 2015. 12588, 12591

Friedrich, J., Janssen, F., Aleynik, D., Bange, H. W., Boltacheva, N., Çagatay, M. N., Dale, A. W., Etiope, G., Erdem, Z., Geraga, M., Gilli, A., Gomoiu, M. T., Hall, P. O. J., Hansson, D., He, Y., Holtappels, M., Kirf, M. K., Kononets, M., Konovalov, S., Lichtschlag, A., Livingstone, D. M., Marinaro, G., Mazlumyan, S., Naeher, S., North, R. P., Papatheodorou, G., Pfannkuche, O., Prien, R., Rehder, G., Schubert, C. J., Soltwedel, T., Sommer, S., Stahl, H., Stanev, E. V., Teaca, A., Tengberg, A., Waldmann, C., Wehrli, B., and Wenzhöfer, F.: Investigating hypoxia in aquatic environments: diverse approaches to addressing a complex phenomenon, Biogeosciences, 11, 1215–1259, doi:10.5194/bg-11-1215-2014, 2014. 12547, 12548

Greenwood, N., Parker, E. R., Fernand, L., Sivyer, D. B., Weston, K., Painting, S. J., Kröger, S., Forster, R. M., Lees, H. E., Mills, D. K., and Laane, R. W. P. M.: Detection of low bottom water oxygen concentrations in the North Sea; implications for monitoring and assessment of ecosystem health, Biogeosciences, 7, 1357–1373, doi:10.5194/bg-7-1357-2010, 2010. 12546, 12548, 12549, 12556, 12560, 12568, 12584, 12586, 12587

Gröger, M., Maier-Reimer, E., Mikolajewicz, U., Moll, A., and Sein, D.: NW European shelf under climate warming: implications for open ocean – shelf exchange, primary production, and carbon absorption, Biogeosciences, 10, 3767–3792, doi:10.5194/bg-10-3767-2013, 2013. 12591

Heath, M., Edwards, A., Pätsch, J., and Turrell, W.: Modelling the Behaviour of Nutrients in the Coastal Waters of Scotland, Scottish Executive Central Research Unit, Edinburgh, 2002. 12553

Jickells, T.: Nutrient biogeochemistry of the coastal zone, Science, 281, 217–222, doi:10.1126/science.281.5374.217, 1998. 12547

Justić, D., Turner, R., and Rabalais, N.: Climatic influences on riverine nitrate flux: implications for coastal marine eutrophication and hypoxia, Estuaries, 26, 1–11, doi:10.1007/BF02691688, 2003. 12591

Kalnay, E., Kanamitsu, M., Kistler, R., Collins, W., Deaven, D., Gandin, L., Iredell, M., Saha, S., White, G., Woollen, J., Zhu, Y., Chelliah, M., Ebisuzaki, W., Higgins, W., Janowiak, J., Mo, K., Ropelewski, C., Wang, J., Leetmaa, A., Reynolds, R., Jenne, R., and Joseph, D.: The NCEP/NCAR 40-year reanalysis project, B. Am. Meteorol. Soc., 77, 437–471, doi:10.1175/1520-0477(1996)077<0437:TNYRP>2.0.CO;2, 1996. 12552

BGD
12, 12543–12610, 2015

Kara, A., Rochford, P., and Hurlburt, H.: An optimal definition for ocean mixed layer depth, J. Geophys. Res.-Oceans, 105, 16803–16821, doi:10.1029/2000JC900072, 2000. 12558
Kemp, W. M., Testa, J. M., Conley, D. J., Gilbert, D., and Hagy, J. D.: Temporal responses of coastal hypoxia to nutrient loading and physical controls, Biogeosciences, 6, 2985–3008, doi:10.5194/bg-6-2985-2009, 2009. 12547, 12568
Kistler, R., Collins, W., Saha, S., White, G., Woollen, J., Kalnay, E., Chelliah, M., Ebisuzaki, W., Kanamitsu, M., Kousky, V., van den Dool, H., Jenne, R., and Fiorino, M.: The NCEP-NCAR 50-year reanalysis: monthly means CD-ROM and documentation, B. Am. Meterorol. Soc., 82, 247–267, doi:10.1175/1520-0477(2001)082<0247:TNNYRM>2.3.CO;2, 2001. 12552
Kröncke, I. and Knust, R.: The Dogger Bank: a special ecological region in the central North Sea, Helgoland. Mar. Res., 49, 335–353, doi:10.1007/BF02368361, 1995. 12546
Lenhart, H.-J. and Pohlmann, T.: The ICES-boxes approach in relation to results of a North Sea circulation model, Tellus A, 49, 139–160, doi:10.1034/j.1600-0870.1997.00010.x, 1997. 12546, 12550
Lenhart, H.-J., Mills, D., Baretta-Bekker, H., van Leeuwen, S., van der Molen, J., Baretta, J., Blaas, M., Desmit, X., Kühn, W., Lacroix, G., Los, H., Ménesguen, A., Neves, R., Proctor, R., Ruardij, P., Skogen, M., Vanhoutte-Brunier, A., Villars, M., and Wakelin, S.: Predicting the consequences of nutrient reduction on the eutrophication status of the North Sea, J. Marine Syst., 81, 148–170, doi:10.1016/j.jmarsys.2009.12.014, 2010. 12552, 12555, 12578, 12590
Lohse, L., Kloosterhuis, H., van Raaphorst, W., and Helder, W.: Denitrification rates as measured by the isotope pairing method and by the acetylene inhibition technique in continental shelf sediments of the North Sea, Mar. Ecol.-Prog. Ser., 132, 169–179, 1996. 12584
Lorkowski, I., Pätsch, J., Moll, A., and Kühn, W.: Interannual variability of carbon fluxes in the North Sea from 1970 to 2006 – Competing effects of abiotic and biotic drivers on the gas-exchange of CO_2, Estuar. Coast. Shelf S., 100, 38–57, doi:10.1016/j.ecss.2011.11.037, 2012. 12550, 12552, 12553
Lowe, J., Howard, T., Pardaens, A., Tinker, J., Holt, J., Wakelin, S., Milne, G., Leake, J., Wolf, J., Horsburgh, K., Reeder, T., Jenkins, G., Ridley, J., Dye, S., and Bradley, S.: UK Climate Projections Science Report: Marine and Coastal Projections, Tech. rep., Met Office Hadley Centre, Exeter, UK, available at: http://nora.nerc.ac.uk/9734/, accessed 29 June 2015, 2009. 12591
Meire, L., Soetaert, K. E. R., and Meysman, F. J. R.: Impact of global change on coastal oxygen dynamics and risk of hypoxia, Biogeosciences, 10, 2633–2653, doi:10.5194/bg-10-2633-2013, 2013. 12588, 12591

BGD
12, 12543–12610, 2015

Neumann, T.: Towards a 3D-ecosystem model of the Baltic Sea, J. Marine Syst., 25, 405–419, doi:10.1016/S0924-7963(00)00030-0, 2000. 12572
O'Boyle, S. and Nolan, G.: The influence of water column stratification on dissolved oxygen levels in coastal and shelf waters around Ireland, Biol. Environ., 110B, 195–209, doi:10.3318/BIOE.2010.110.3.195, 2010. 12546
O'Driscoll, K., Mayer, B., Ilyina, T., and Pohlmann, T.: Modelling the cycling of persistent organic pollutants (POPs) in the North Sea system: fluxes, loading, seasonality, trends, J. Marine Syst., 111, 69–82, doi:10.1016/j.jmarsys.2012.09.011, 2013. 12552
OSPAR-Commission: OSPAR integrated report 2003 on the eutrophication status of the OSPAR maritime area based upon the first application of the Comprehensive Procedure, London, 2003. 12547
OSPAR-Commission: Common procedure for the identification of the eutrophication status of the OSPAR maritime area, London, 2005. 12567, 12572
Otto, L., Zimmerman, J., Furnes, G., Mork, M., Saetre, R., and Becker, G.: Review of the physical oceanography of the North Sea, Neth. J. Sea Res., 26, 161–238, doi:10.1016/0077-7579(90)90091-T, 1990. 12546
Pätsch, J. and Kühn, W.: Nitrogen and carbon cycling in the North Sea and exchange with the North Atlantic – a model study. Part I. Nitrogen budget and fluxes, Cont. Shelf Res., 28, 767–787, doi:10.1016/j.csr.2007.12.013, 2008. 12550, 12551, 12552
Pingree, R., Holligan, P., and Mardell, G.: The effects of vertical stability on phytoplankton distributions in the summer on the northwest European Shelf, Deep-Sea Res., 25, 1011–1016, doi:10.1016/0146-6291(78)90584-2, 1978. 12546, 12547, 12567
Pohlmann, T.: Untersuchung hydro- und thermodynamischer Prozesse in der Nordsee mit einem dreidimensionalen numerischem Modell, Berichte aus dem Zentrum für Meeres- und Klimaforschung, Reihe B, Zentrum für Meeres- und Klimaforschung der Universität Hamburg, Hamburg, 1–116, 1991. 12550
Pohlmann, T.: Predicting the thermocline in a circulation model of the North Sea – Part I: model description, calibration and verification, Cont. Shelf Res., 16, 131–146, doi:10.1016/0278-4343(95)90885-S, 1996. 12550
Queste, B., Fernand, L., Jickells, T., and Heywood, K.: Spatial extent and historical context of North Sea oxygen depletion in August 2010, Biogeochemistry, 113, 53–68, doi:10.1007/s10533-012-9729-9, 2013. 12547, 12548, 12568, 12585, 12588

BGD
12, 12543–12610, 2015

Rabalais, N. N., Díaz, R. J., Levin, L. A., Turner, R. E., Gilbert, D., and Zhang, J.: Dynamics and distribution of natural and human-caused hypoxia, Biogeosciences, 7, 585–619, doi:10.5194/bg-7-585-2010, 2010. 12547, 12588, 12591

Rachor, E. and Albrecht, H.: Sauerstoff-Mangel im Bodenwasser der Deutschen Bucht, Veröff. Inst. Meeresforsch. Bremerh., 19, 209–227, 1983. 12547

Reinthaler, T., Bakker, K., Manuels, R., Van Ooijen, J., and Herndl, G.: Fully automated spectrophotometric approach to determine oxygen concentrations in seawater via continuous-flow analysis, Limnol. Oceanogr.-Meth., 4, 358–366, doi:10.4319/lom.2006.4.358, 2006. 12557

Salt, L., Thomas, H., Prowe, A., Borges, A., Bozec, Y., and de Baar, H.: Variability of North Sea pH and CO_2 in response to North Atlantic Oscillation forcing, J. Geophys. Res.-Biogeo., 118, 1584–1592, doi:10.1002/2013JG002306, 2013. 12557

Schernewski, G., Friedland, R., Carstens, M., Hirt, U., Leujak, W., Nausch, G., Neumann, T., Petenati, T., Sagert, S., Wasmund, N., and von Weber, M.: Implementation of European marine policy: new water quality targets for German Baltic waters, Mar. Policy, 51, 305–321, doi:10.1016/j.marpol.2014.09.002, 2015. 12591

Schöpp, W., Posch, M., Mylona, S., and Johansson, M.: Long-term development of acid deposition (1880–2030) in sensitive freshwater regions in Europe, Hydrol. Earth Syst. Sci., 7, 436–446, doi:10.5194/hess-7-436-2003, 2003. 12554

Seitzinger, S. and Giblin, A.: Estimating denitrification in North Atlantic continental shelf sediments, Biogeochemistry, 35, 235–260, 1996. 12551

Steele, J.: Environmental control of photosynthesis in the sea, Limnol. Oceanogr., 7, 137–150, doi:10.4319/lo.1962.7.2.0137, 1962. 12550

Taylor, K.: Summarizing multiple aspects of model performance in a single diagram, J. Geophys. Res.-Atmos., 106, 7183–7192, 2001. 12565

Thomas, H., Bozec, Y., Elkalay, K., de Baar, H. J. W., Borges, A. V., and Schiettecatte, L.-S.: Controls of the surface water partial pressure of CO_2 in the North Sea, Biogeosciences, 2, 323–334, doi:10.5194/bg-2-323-2005, 2005. 12564

Topcu, H.D. and Brockmann, U.H.: Seasonal oxygen depletion in the North Sea, a review, Mar. Pollut. Bull., doi:10.1016/j.marpolbul.2015.06.021, 2015. 12601

Topcu, D., Brockmann, U., and Claussen, U.: Relationship between eutrophication reference conditions and boundary settings considering OSPAR recommendations and the Water

BGD
12, 12543–12610, 2015

Framework Directive – examples from the German Bight, Hydrobiologia, 629, 91–106, doi:10.1007/s10750-009-9778-9, 2009. 12547, 12591

Troost, T., Blaas, M., and Los, F.: The role of atmospheric deposition in the eutrophication of the North Sea: a model analysis, J. Marine Syst., 125, 101–112, doi:10.1016/j.jmarsys.2012.10.005, 2013. 12590

Upton, A., Nedwell, D., Parkes, R., and Harvey, S.: Seasonal benthic microbial activity in the southern North Sea; oxygen uptake and sulphate reduction, Mar. Ecol.-Prog. Ser., 101, 273–281, doi:10.3354/meps101273, 1993. 12581

v. Westernhagen, H., Hickel, W., Bauerfeind, E., Niermann, U., and Kröncke, I.: Sources and effects of oxygen deficiencies in the south-eastern North Sea, Ophelia, 26, 457–473, doi:10.1080/00785326.1986.10422006, 1986. 12547

van der Molen, J., Aldridge, J., Coughlan, C., Parker, E., Stephens, D., and Ruardij, P.: Modelling marine ecosystem response to climate change and trawling in the North Sea, Biogeochemistry, 113, 213–236, doi:10.1007/s10533-012-9763-7, 2013. 12591

van Leeuwen, S., Tett, P., Mills, D., and van der Molen, J.: Stratified and non-stratified areas in the North Sea: long-term variability and biological and policy implications, J. Geophys. Res.-Oceans, 120, doi:10.1002/2014JC010485, 2015. 12546, 12567

Wanninkhof, R.: Relationship between wind speed and gas exchange, J. Geophys. Res., 97, 7373–7382, doi:10.1029/92JC00188, 1992. 12551

Weston, K., Fernand, L., Nicholls, J., Marca-Bell, A., Mills, D., Sivyer, D., and Trimmer, M.: Sedimentary and water column processes in the Oyster Grounds: a potentially hypoxic region of the North Sea, Mar. Environ. Res., 65, 235–249, doi:10.1016/j.marenvres.2007.11.002, 2008. 12584, 12591

BGD
12, 12543–12610, 2015

Table 1. Critical quantities characterising the O_2 dynamics in the 4 different 4×4-regions (see Fig. 2, yellow boxes). Fluxes are cumulated over the given period and relate to a surface layer of thickness D_{ref} = 25 m.

region		A – SNS		B – SCNS		C – NCNS		D – NNS	
integration period		year	summer	year	summer	year	summer	year	summer
PP_{mld}	$gC\,m^{-2}$	192.1	169.0	178.0	147.8	153.0	134.6	164.3	148.1
$ADH_{org,in}$	$gC\,m^{-2}$	143.1	95.9	165.9	109.2	119.5	92.3	139.6	111.0
$ADH_{org,out}$	$gC\,m^{-2}$	133.3	89.2	165.3	107.6	122.5	92.7	145.0	114.4
EXP_{org}	$gC\,m^{-2}$	27.8	23.4	21.4	17.5	19.3	16.2	21.5	18.4
MIX_{O_2}	$gO_2\,m^{-2}$	230.7	116.1	182.1	66.7	208.5	13.7	217.5	18.2
initial O_2	$mgO_2\,L^{-1}$	9.3	10.1	9.1	9.9	8.9	9.5	9.0	9.5
initial $O_{2,sat}$	$mgO_2\,L^{-1}$	11.5	12.1	11.2	11.9	11.0	11.5	11.2	11.6
area	km^{-2}	7643.1		7454.3		7108.9		6677.2	
V_{sub}	km^{-3}	111.2		137.9		483.2		590.5	

BGD
12, 12543–12610, 2015

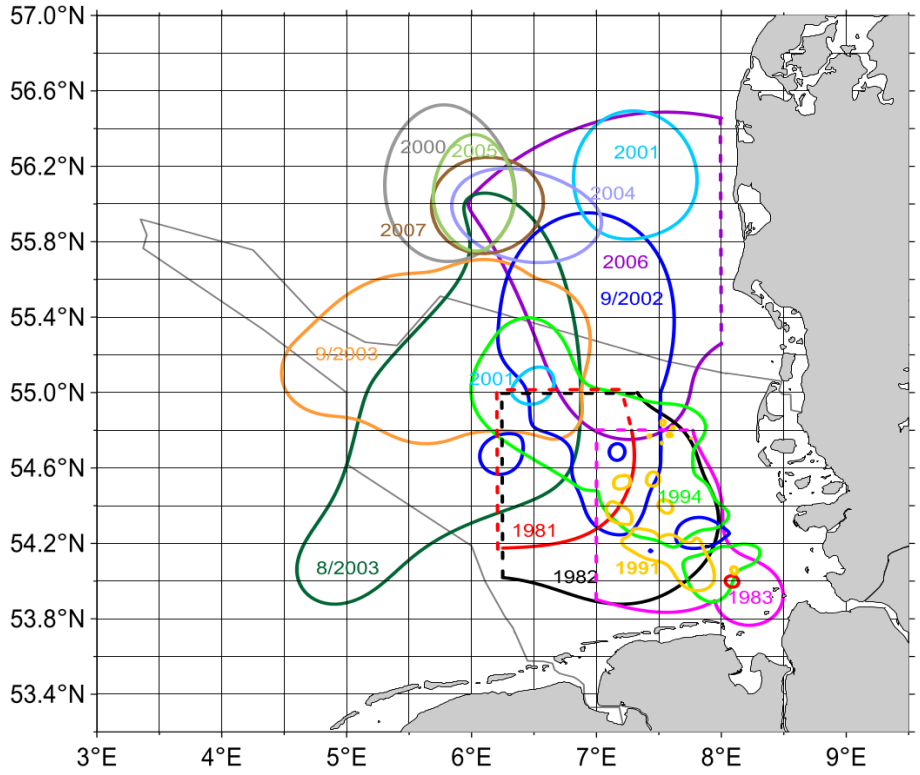

Figure 1. Extent of observed O_2 concentrations < 6 mg L^{-1} in the German Bight area from 1980 to 2010. Survey limitations are indicated by dotted lines. Light grey line marks German Maritime Area (from Topcu and Brockmann , 2015).

BGD
12, 12543–12610, 2015

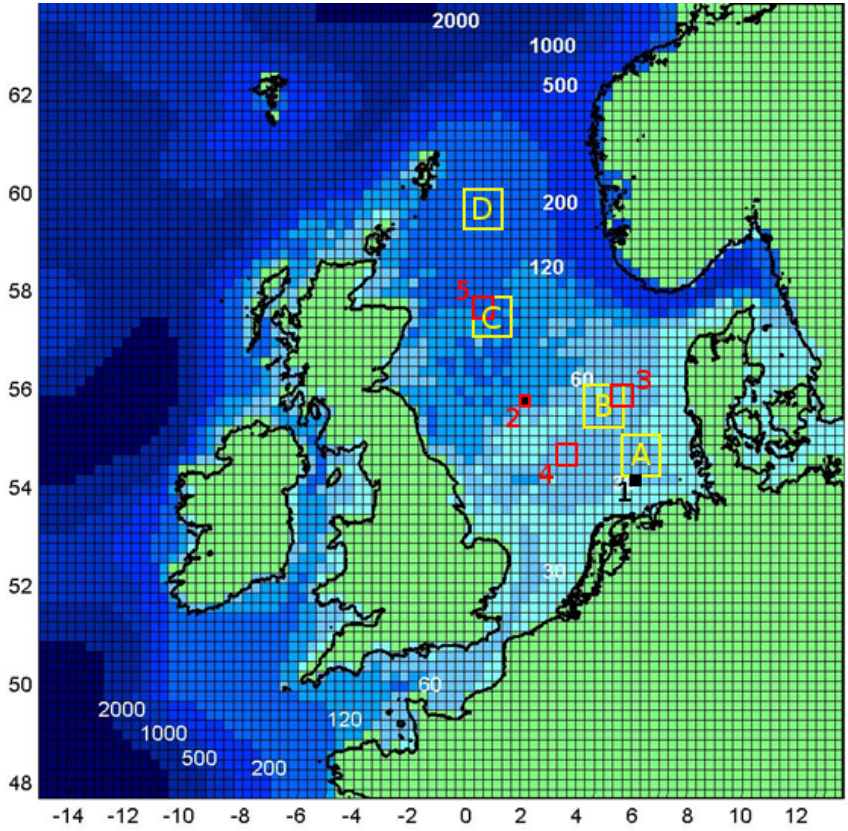

Figure 2. Horizontal grid and bottom topography of the HAMSOM-ECOHAM5 model domain. White numbers indicate depth levels. Yellow boxes A–D mark the 4×4-regions used for the characterisation of key features presented in Sect. 3.4. Black-filled boxes (1, 2) mark the validation sites discussed in Sect. 3.2.1 Red-framed boxes (2–5) indicate regions used for the O_2 mass balance calculations in Sects. 3.5–3.8.

BGD
12, 12543–12610, 2015

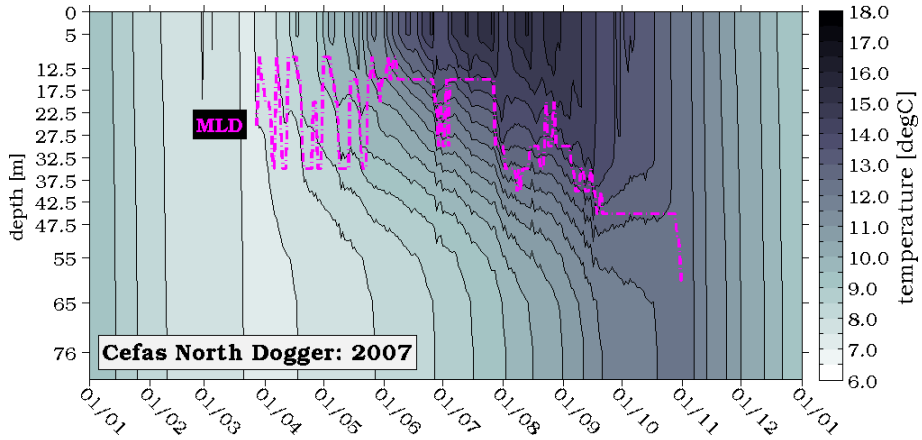

Figure 3. Hovmöller diagram of simulated T and MLD according to Eqs. (1) and (2) at Cefas station North Dogger (see Fig. 2, region 2) in 2007. Depth levels represent the centre depth of model layers.

BGD
12, 12543–12610, 2015

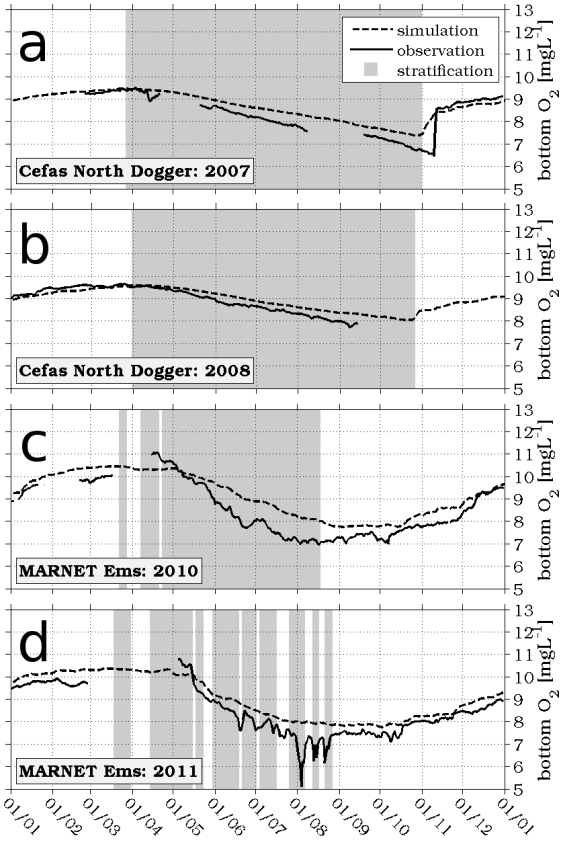

Figure 4. Annual time series of observed and simulated bottom O_2 concentration at Cefas station North Dogger in **(a)** 2007 and **(b)** 2008, and at MARNET station Ems in **(c)** 2010 and **(d)** 2011. Same legend for all panels.

BGD
12, 12543–12610, 2015

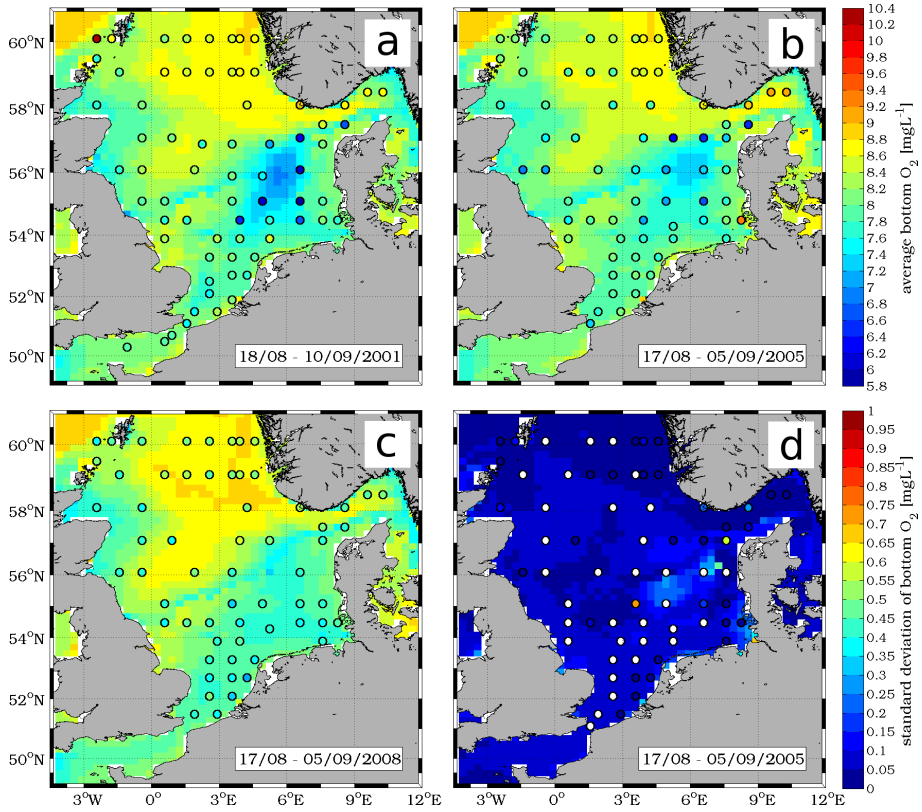

Figure 5. Spatial distribution of observed and simulated average bottom O_2 concentration in late summer **(a)** 2001, **(b)** 2005 and **(c)** 2008, and **(d)** standard deviation in 2005. Colour scale of panel **(b)** applies to panels **(a–c)**. Circles indicate sample sites, underlying colours show simulation results. Averages and standard deviation were calculated for the whole observation period (bottom-left corner of each panel). White circles in **(d)** mark model bottom grid cells with only one corresponding observed value (i.e. no standard deviation).

BGD
12, 12543–12610, 2015

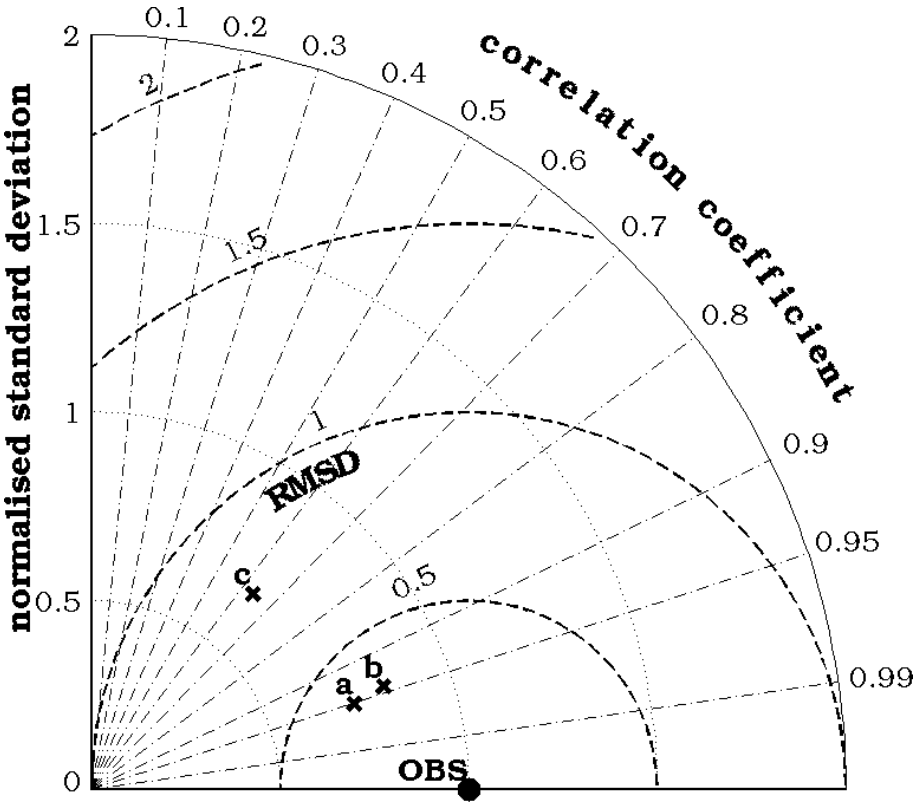

Figure 6. Taylor diagram of simulated (×) bottom O_2 concentration compared to observations (OBS) for time series (see Fig. 4) at **(a)** Cefas North Dogger and **(b)** MARNET Ems, and **(c)** spatially resolved data (see Fig. 5). Standard deviations and centred root-mean-square differences (RMSD) were normalised by the standard deviation of the corresponding observations.

BGD
12, 12543–12610, 2015

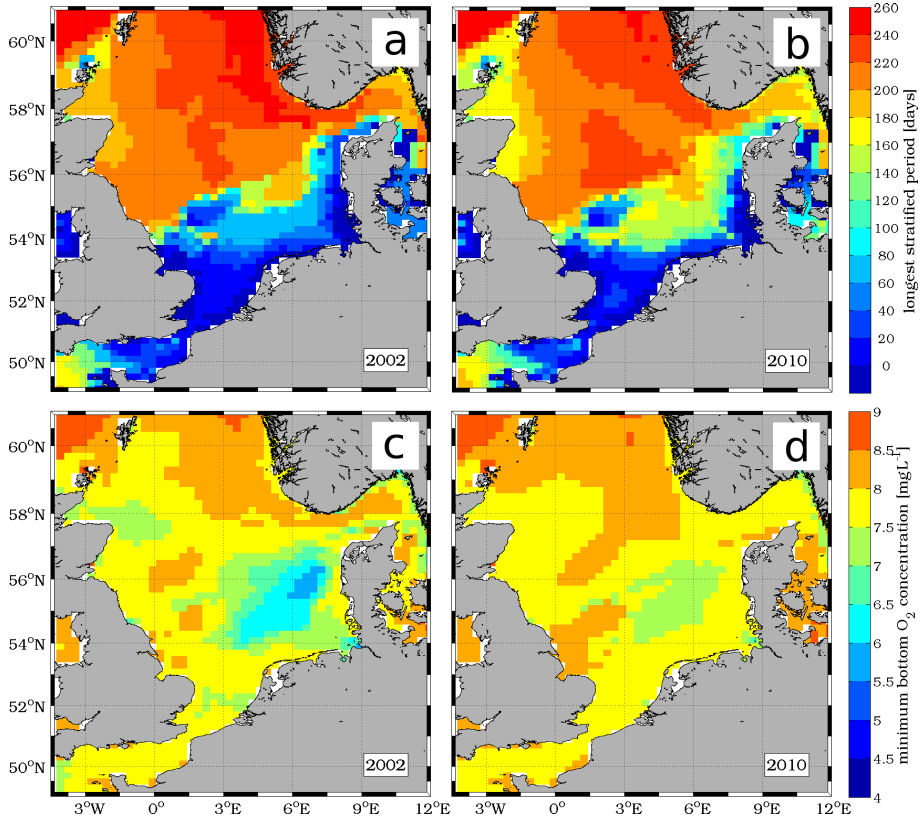

Figure 7. Spatial distributions of **(a, b)** longest continuous stratification period derived from simulated T according to Eq. (1) and **(c, d)** simulated annual minimum bottom O_2 concentration for the years 2002 **(a, c)** and 2010 **(b, d)**. Same colour scales for **(a, b)**, and **(c, d)**.

BGD
12, 12543–12610, 2015

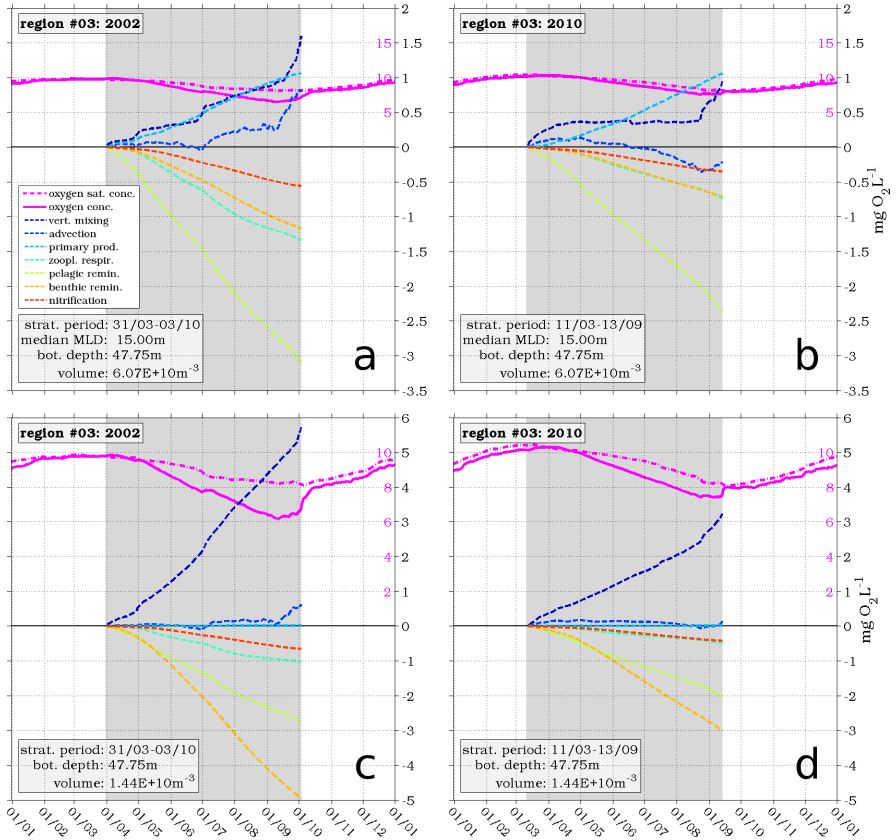

Figure 8. Mass balances of simulated O_2 in region 3 (see Fig. 2) during the stratified period: **(a, b)** for the whole volume below the annual median MLD (according to Eq. 2), and **(c, d)** only for the bottom layer for the years 2002 **(a, c)** and 2010 **(b, d)**. Same legend for all panels. Magenta *y* axis applies to O_2 (saturation) concentration. Changes in concentration due to different processes are cumulative. Text boxes list relevant stratification parameters, bottom depth and volume of the analysed water body. Note different *y* axis for **(a–d)**.

BGD
12, 12543–12610, 2015

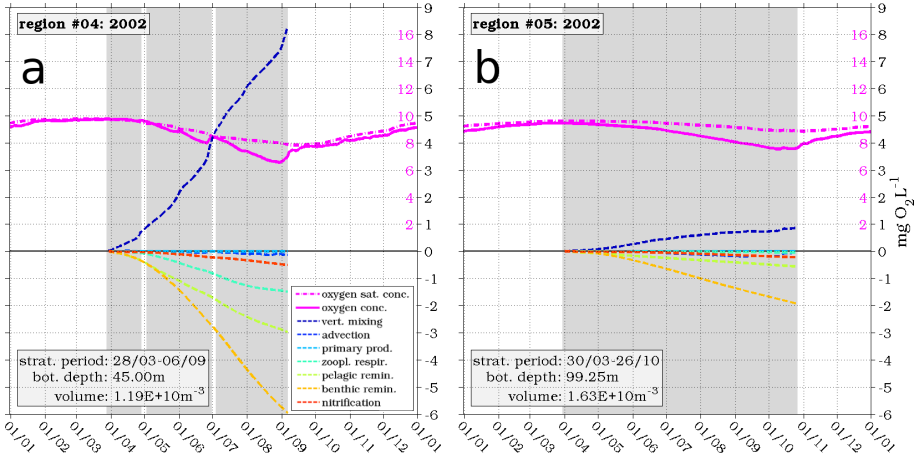

Figure 9. Mass balances of simulated bottom O_2 in regions 4 **(a)** and 5 **(b)**; (see Fig. 2) during the stratified period in 2002. Same legend for **(a, b)**. Magenta *y* scale applies to O_2 (saturation) concentration. Changes in concentration due to different processes are cumulative.

BGD
12, 12543–12610, 2015

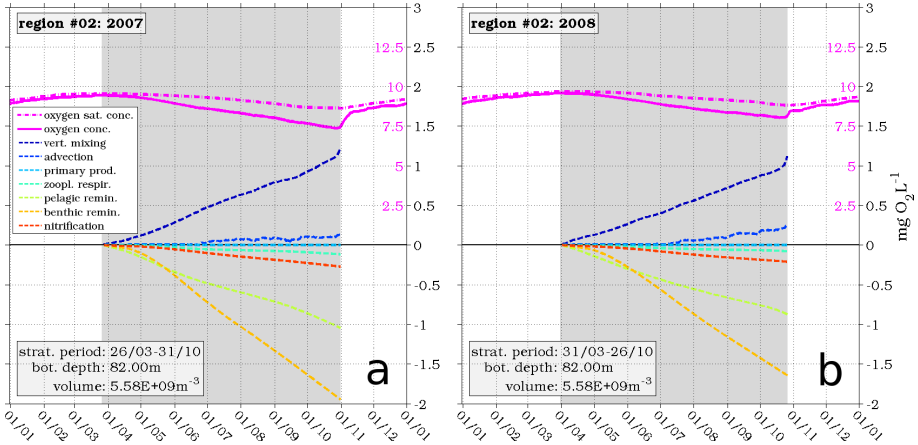

Figure 10. Mass balances for simulated bottom O_2 at Cefas North Dogger (see Fig. 2, region 2) during the stratified period in **(a)** 2007 and **(b)** 2010. Same legend for **(a, b)**. Magenta *y* scale applies to O_2 (saturation) concentration. Changes in concentration due to different processes are cumulative.

BGD
12, 12543–12610, 2015